GEORGIA DOT RESEARCH PROJECT 15-01

FINAL REPORT

Hurricane Vulnerability Assessment of Coastal Bridges in Georgia

OFFICE OF RESEARCH
15 KENNEDY DRIVE
FOREST PARK, GA 30297

1.Report No.: FHWA-GA-17-15-01	2. Government Accession No.:	3. Recipient's Catalog No.:	
4. Title and Subtitle: Hurricane Vulnerability Assessment of Coastal Bridges in Georgia		5. Report Date: July 2017	
		6. Performing Organization Code:	
7. Author(s): Chorzepa, Mi G. (PI), Stephan A. Durham (Co-PI), Jason Christian (Co-PI)		8. Performing Organ. Report No.: 15-01	
9. Performing Organization Name and Address: The University of Georgia Driftmier Engineering Center Athens, GA30602		10. Work Unit No.:	
		11. Contract or Grant No.: RP 15-01 PI# 0013541	
12. Sponsoring Agency Name and Address: Georgia Department of Transportation Office of Performance-based Management and Research 15 Kennedy Drive Forest Park, GA 30297-2534		13. Type of Report and Period Covered: Final; June 2015 – June 2017	
		14. Sponsoring Agency Code:	
15. Supplementary Notes:			
16. Abstract: This report presents the recommendations for coastal bridges potentially vulnerable to hurricane events for the Georgia Department of Transportation (GDOT). The main goal of this research was to evaluate potential hurricane hazard to coastal bridges from wave forces. It has been observed during past hurricanes that bridges located in the coastal environment are vulnerable to deck shifting/unseating due to wave forces. It is recommended through this study that coastal bridges be elevated in the future and that dowel connections should be considered in conjunction with external restrainers to reduce the vulnerability. This research provides an improved understanding of vulnerable bridge elements as well as further insight into preventing and mitigating damage that can occur during a major hurricane event.			
17. Key Words: Vulnerability, Coastal, Bridge, Hurricane, Fragility, Anchor bolt, Dowel, Probability		18. Distribution Statement:	
19. Security Classification (of this report): Unclassified	20. Security Classification (of this page): Unclassified	21. Number of Pages: 106	22. Price:

Form DOT 1700.7 (8-69)

SI* (MODERN METRIC) CONVERSION FACTORS

APPROXIMATE CONVERSIONS TO SI UNITS

Symbol	When You Know	Multiply By	To Find	Symbol
		LENGTH		
in	inches	25.4	millimeters	mm
ft	feet	0.305	meters	m
yd	yards	0.914	meters	m
mi	miles	1.61	kilometers	km
		AREA		
in^2	square inches	645.2	square millimeters	mm^2
ft^2	square feet	0.093	square meters	m^2
yd^2	square yard	0.836	square meters	m^2
ac	acres	0.405	hectares	ha
mi^2	square miles	2.59	square kilometers	km^2
		VOLUME		
fl oz	fluid ounces	29.57	milliliters	mL
gal	gallons	3.785	liters	L
ft^3	cubic feet	0.028	cubic meters	m^3
yd^3	cubic yards	0.765	cubic meters	m^3
		NOTE: volumes greater than 1000 L shall be shown in m^3		
		MASS		
oz	ounces	28.35	grams	g
lb	pounds	0.454	kilograms	kg
T	short tons (2000 lb)	0.907	megagrams (or "metric ton")	Mg (or "t")
		TEMPERATURE (exact degrees)		
°F	Fahrenheit	5 (F-32)/9 or (F-32)/1.8	Celsius	°C
		ILLUMINATION		
fc	foot-candles	10.76	lux	lx
fl	foot-Lamberts	3.426	$candela/m^2$	cd/m^2
		FORCE and PRESSURE or STRESS		
lbf	poundforce	4.45	newtons	N
lbf/in^2	poundforce per square inch	6.89	kilopascals	kPa

APPROXIMATE CONVERSIONS FROM SI UNITS

Symbol	When You Know	Multiply By	To Find	Symbol
		LENGTH		
mm	millimeters	0.039	inches	in
m	meters	3.28	feet	ft
m	meters	1.09	yards	yd
km	kilometers	0.621	miles	mi
		AREA		
mm^2	square millimeters	0.0016	square inches	in^2
m^2	square meters	10.764	square feet	ft^2
m^2	square meters	1.195	square yards	yd^2
ha	hectares	2.47	acres	ac
km^2	square kilometers	0.386	square miles	mi^2
		VOLUME		
mL	milliliters	0.034	fluid ounces	fl oz
L	liters	0.264	gallons	gal
m^3	cubic meters	35.314	cubic feet	ft^3
m^3	cubic meters	1.307	cubic yards	yd^3
		MASS		
g	grams	0.035	ounces	oz
kg	kilograms	2.202	pounds	lb
Mg (or "t")	megagrams (or "metric ton")	1.103	short tons (2000 lb)	T
		TEMPERATURE (exact degrees)		
°C	Celsius	1.8C+32	Fahrenheit	°F
		ILLUMINATION		
lx	lux	0.0929	foot-candles	fc
cd/m^2	$candela/m^2$	0.2919	foot-Lamberts	fl
		FORCE and PRESSURE or STRESS		
N	newtons	0.225	poundforce	lbf
kPa	kilopascals	0.145	poundforce per square inch	lbf/in^2

*SI is the symbol for the International System of Units. Appropriate rounding should be made to comply with Section 4 of ASTM E380.
(Revised March 2003)

GDOT Research Project No. 15-01

Final Report

Hurricane Vulnerability Assessment of Coastal Bridges in Georgia

Prepared by

Mi G. Chorzepa, Ph.D., P.E.
Assistant Professor
Civil Engineering, College of Engineering
University of Georgia

Jason Christian, Ph.D., P.E.
Assistant Professor
Environmental Engineering, College of Engineering
University of Georgia

Stephan Durham, Ph.D., P.E.
Associate Professor
Civil Engineering, College of Engineering
University of Georgia

Contract with
Georgia Department of Transportation

In cooperation with
U.S. Department of Transportation
Federal Highway Administration

July 2017

DISCLAIMER

The contents of this report reflect the views of the authors, who are solely responsible for the facts and accuracy of the data, the opinions, and the conclusions presented herein. The contents do not necessarily reflect the official view or policies of the Georgia Department of Transportation (GDOT) and Federal Highway Administration (FHWA). This report does not constitute a standard, specification, or regulation, and its contents are not intended for construction, bidding, or permit purposes. The use of names or specific products or manufacturers listed herein does not imply endorsement of those products or manufacturers.

ACKNOWLEDGMENTS

The University of Georgia would like to acknowledge the financial support provided by the Georgia Department of Transportation for this study. The authors would like to gratefully acknowledge the contributions of many individuals to the successful completion of this research project. This especially includes Mr. Ben Rabun (retired technical manager), Mr. Andy Doyle (Bridge Maintenance), Mr. Clayton Bennett (Bridge Maintenance), Mr. Chales Aziabor (Bridge Maintenance), Mr. David Jared (Research), and Mark Demidovich (TMC) who have helped the research team by coordinating field investigations and reviewing bridges plans with research team, and Mr. Bill DuVall (Bridge Design), who met with the team during the project implementation workshop and provided valuable comments.

Special thanks to our research project manager, Mr. Binh Bui, for sharing resources and coordinating numerous meetings with the Bridge Maintenance Unit, Transportation Management Center, and Bridge Design office. This report presents some of the results from PhD dissertation (August 2017) of Arash Saeidpour who was financially supported by this project. He dedicated his time to studying methodologies that yielded the findings and recommendations presented herein. Furthermore, special thanks to our undergraduate assistants, Gregory Coughlin, Jonathan Chelena, and Adara Darson and a Young Dawgs intern, Ryan Iyer, who have contributed to this project. Finally, the authors are conducting a beyond design-basis wind analysis of two cable-stayed bridges located along the Georgia coastline although it is beyond the scope of this study. The analysis results will be available in Maximillian Ovett's MS thesis in December 2017.

EXECUTIVE SUMMARY

The Georgia Department of Transportation (GDOT) can anticipate the hurricane vulnerability of its coastal bridge structures, allocate available resources for the most needed hurricane preparedness and recovery effort, and prepare the state with a transportation infrastructure that is less susceptible to hurricane impact.

This report presents the recommendations for coastal bridges potentially vulnerable to hurricane events for the Georgia Department of Transportation (GDOT). The main goal of this research was to evaluate potential hurricane hazard to coastal bridges from wave forces. It has been observed during past hurricanes that bridges located in the coastal environment are vulnerable to deck shifting/unseating due to wave forces. It is recommended through this study that coastal bridges be elevated in the future and that dowel connections should be considered in conjunction with external restrainers to reduce the hurricane vulnerability. This research provides an improved understanding of vulnerable bridge elements as well as further insight into preventing and mitigating damage that can occur during a major hurricane event.

The study team has completed initial and secondary level analyses (i.e., Level I and Level II) in accordance with the AASHTO Guide Specifications for Bridges Vulnerable to Coastal Storms (2008) and assessed a likelihood of hurricane-induced damage in coastal bridges for Hurricane Category 1 through 5 events. The study findings from initial screening, Level-I analysis, and Level-II assessment are presented in Sections 4, 5, and 6, respectively.

By analyzing the outcomes of this study, the study team has identified coastal bridges which are at greatest risk of damage, as well as bridge components which are vulnerable to hurricanes. Based on the experience of conducting a hurricane vulnerability evaluation using the AASHTO Guide Specification, it is recommended for GDOT's adoption as the AASHTO Guide for Georgia's critically important coastal bridges, with the following recommendations:

- It should be recognized that the AASHTO Guide (Level I and II methods) procedures yield a conservative assessment of wave forces; and

- It is highly recommended that a Level-III analysis be conducted to accurately quantify the wave forces and consider specific hurricanes that are probable to form in the Atlantic coast.

The parameters necessary for implementation of the research findings in the 'BridgeWatch' software are organized in excel format (Section 7.1). A master database, including bridge parameters extracted from plans, used for this study is prepared for GDOT's future use (Section 7.2). Finally, the research findings are organized using the 'ArcMap' software (Section 7.3) for a graphical presentation and thus to enhance communication and user-friendliness.

It is concluded from this study that a majority of bridges with dowel connections between super- and sub-structures are vulnerable to hurricane hazards. It is recommended that external restrainers and/or shear keys be considered and that other connection types and bridge elements be studied to reduce and/or mitigate the vulnerability. It is also recommended that coastal bridges be continuously monitored during and after future hurricane events.

It is finally recommended that all construction documents be efficiently archived and easily accessible when vulnerability assessments are conducted. This includes: all design and construction drawings, particularly pertaining to super- and sub-structure connections, rehabilitation history, and other construction information.

TABLE OF CONTENTS

LIST OF TABLES

LIST OF FIGURES

ABBREVIATIONS LIST

Abbreviation	
AASHTO	American Association of State Highway and Transportation Officials
ASCE	American Society of Civil Engineers
Caltrans	California Department of Transportation
DOT	Department of Transportation
FHWA	Federal Highway Administration
GEMA	Georgia Emergency Management Agency
GDOT	Georgia Department of Transportation
GIS	Geographic Information System
IM	Intensity Measure
MOM	Maximum of Maximum
NBI	National Bridge Inventory
NWS	National Weather Service
NOAA	National Oceanic and Atmospheric Administration
NWS	National Weather Service
SLOSH	Sea, Lake, and Overland Surges from Hurricane
OpenSees	Open System for Earthquake Engineering Simulation

1. INTRODUCTION

1.1 Background and Recent Hurricanes

Recent U.S. hurricanes including Sandy (New York - 2012), Ike (Houston - 2008), and Katrina (New Orleans - 2005) inflicted direct physical damage of over $180 billion to the coastal communities (NOAA, 2013). Figure 1 shows the flooding of bridge approaches after Katrina (Weather.com 2016). Many other urban communities along the Eastern U.S. and Gulf coasts have learned through experience how vulnerable their transportation infrastructure is to hurricane impacts, but such experience may not be the most efficient way to learn these important lessons.

Furthermore, the natural disaster recovery cost for transportation infrastructure and related social impact are proving to be unsustainable. The Federal Highway Administration's emergency relief program appropriated $224 million for New Jersey's Hurricane Sandy-related repairs to aid in the restoration or reconstruction of bridges and roads (U.S. Department of Transportation, 2013). Hurricane Sandy impaired transportation infrastructure, which prevented residents from driving to work, school, hospital, grocery stores, gas stations, and other places (NYC 2012). Sandy demonstrated shortcomings in the way we (residents/officials) respond to natural disasters.

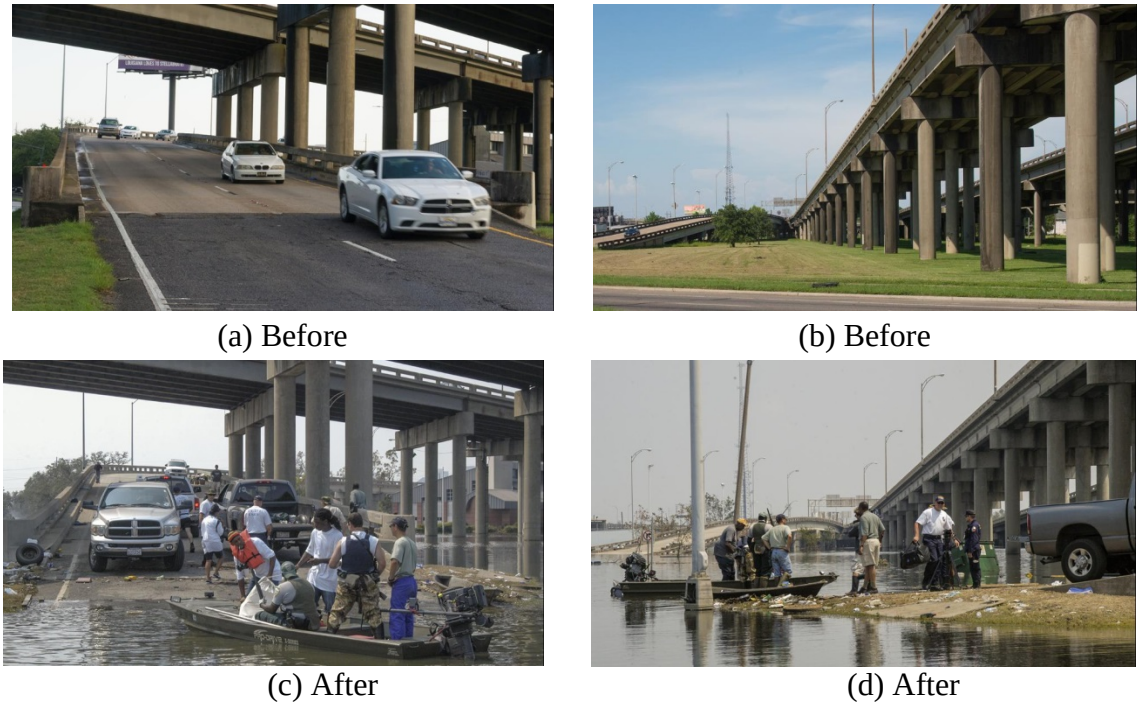

(a) Before (b) Before

(c) After (d) After

Figure 1 – Photos of Highway Bridges (a) Before and (b) After Hurricane Katrina, 2005.

Hurricanes and other severe storms have proven themselves to be one of the major threats to transportation assets throughout the world, particularly to bridges located along the coastlines. There are nearly 96,500 kilometers of roads located along the coastal regions of the United States susceptible to tropical storms and hurricane induced surges and waves (Douglass et al. 2006). Bridges as key components of transportation networks have shown to be one of the most vulnerable assets to these natural hazards. A large number of bridges along the Gulf coast of U.S. suffered severe damage during recent hurricanes such as Ike, Ivan, Katrina, and Rita. These events have raised a national awareness of infrastructure resilience and reliability of transportation networks vulnerable to severe weather events.

For instance, the interstate (I-10) bridge over Escambia Bay in Florida suffered significant damage from Hurricane Ivan in September 2004, resulting in a loss of 63 spans and dislocation of 52 others (Sheppard and Marin 2009). The bridge was closed to traffic for nearly two months. Hurricanes Katrina and Rita in 2005, as two of the most intense Atlantic hurricanes, inflicted devastating damage to highway bridges in Florida, Alabama, Mississippi, Louisiana, and Texas. Some of the major bridges that suffered significant damage from these hurricanes include bridges over Lake Pontchartrain, I-10 twin span bridges, US-11 bridge, Norfolk Southern Railroad bridge, Lake Pontchartrain Toll Causeway, bridges over St. Louis Bay, US-90 bridge, CSX Railroad bridge, bridges over Biloxi Bay and Back Bay, I-110 bridge including ramps, Popps Ferry bridge, and bridges over Mobile Bay (Gutierrez et al. 2006). Figure 2 illustrates the destruction to the bridges inflicted by past hurricanes.

Past events have clearly demonstrated that the economic and social impacts to the community are excruciating (Padgett et al. 2008). Any loss of functionality in transportation networks will hinder the post-event emergency services and recovery efforts in the near term and

will slow down economic and social development of affected regions in the long-run. It has been estimated that there are 36,000 bridges within 28 kilometers of the US coasts, out of which more than 1,000 bridges remain susceptible to similar damage (Douglass and Krolak 2008).

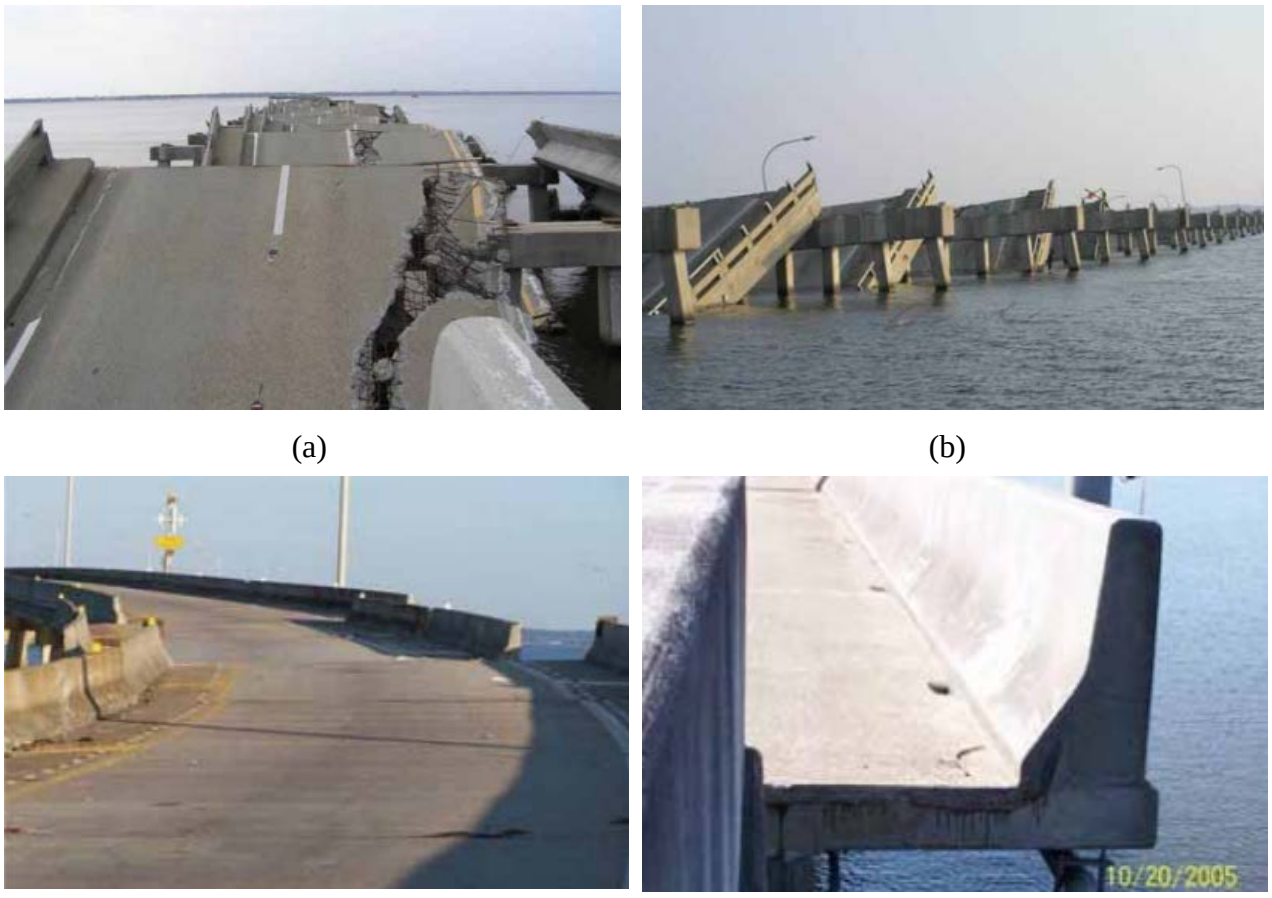

(a) (b)

(c) (d)

Figure 2 – Damage to Bridges Inflicted by Past Hurricanes (Gutierrez et al. 2006).

(a) Displaced superstructure spans of US-90 bridge over St. Louis Bay (photo credit: NIST);

(b)Looking west toward Biloxi from the east shore, many superstructure spans of US-90 Biloxi-Ocean Springs bridge were displaced north off their piers (photo credit: J.O'Connor, MCEER);

(c) Bridge spans pushed north by the surge (photo credit: LA DOT);

(d) Displaced spans of Popps Ferry Bridge (photo credit: J. O'Connor, MCEER).

1.2 Hurricanes in Georgia

Fortunately, Georgia coastal communities have not seen hurricane impact in recent memory. However, Georgia is an extremely vulnerable state to hurricane-related hazards (GEMA 2013), potentially resulting in widespread damage, economic disruptions, and coastal evacuations. Georgia's coastal areas, including the ports at Savannah and Brunswick, play essential roles in Georgia's economic well-being. A Washington-based consulting firm has ranked Georgia Ports' deepening project high on its list of the 100 infrastructure projects that would most help the U.S. regain its competitiveness (Business in Savannah 2013). The reliability of these port facilities and the ground transportation network serving them during severe weather events is becoming increasingly important.

Figure 3 includes two photos to illustrate how vulnerable the coastal Georgia is. The photo in Fig. 3(a) contains a traffic intersection in Chatham County, where the location does not appear to be vulnerable on a normal day. However, the intersection of Johnny Mercer Dr. and Wilmington Island Rd is expected to be completely flooded when Hurricanes reaching Category 3 and higher is considered, as shown in Fig. 3(a). Figure 3(b) shows the city hall building and a road that leads to the city hall on Tybee Inland. A similar storm water elevation rise is expected.

(a) (b)

Figure 3 – Predicted hurricane-induced storm surge elevations in Chatham County, GA

(a) Wilmington Island and (b) Tybee Island (U.S. Army 2009).

1.3 Primary Failure Modes

The FHWA study (Douglass and Krolak 2008), titled 'Highways in Coastal Environment', provides a summary of the likely failure mechanism in coastal bridges during severe hurricane events. The potential failure mechanism includes individual waves producing both vertical uplift force and horizontal forces on a simple-span bridge deck (Douglass and Krolak 2008), which yield deck uplifting and/or unseating as illustrated in Figs. 4(a) and (b). The magnitude of the maximum resultant wave force is able to overcome the weight of the decks and tensile capacity of anchor bolts (see Figs. 4c and d), and/or lateral resistance provided by the connections (Douglass et al. 2006).

(a) Typical Deck Uplifting

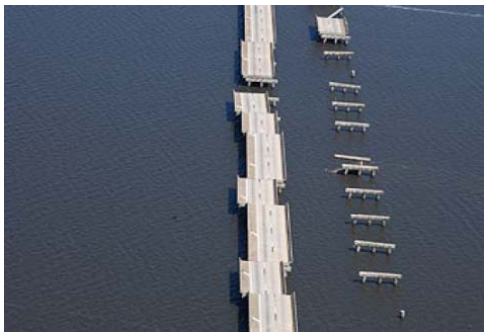

(b) Typical Deck Uplifting/Unseating

(c) Typical Anchor Bot Failure

(d) Typical Connection Failure

Figure 4 – Primary Failure Mode.

(photo credit Douglass et al. 2008; Okeil et al. 2008; and Ataei and Padgett 2008).

Moreover, the primary failure modes and mechanism have been recognized by several studies in the literature. Three most noteworthy quotations are listed below:

(a) Douglass, Scott L., Bret M. Webb, and Roger Kilgore, “Highways in the Coastal Environment: Assessing Extreme Events”, Report No. FHWA-NHI-14-006. 2014:

> “As part of a synthesis of the existing body of knowledge related to wave forces on highway bridge decks Douglass et al. (2006) concluded that wave loads were the primary force causing much of the damage to coastal bridges in the north, central Gulf coast due to Hurricanes Ivan (2004) and Katrina (2005). The likely damage mechanism was waves that struck the simple-span bridge decks because the storm surge raised the water level. The likely failure mechanism was individual waves producing both an uplift force and a horizontal force on the simple-span bridge deck. The magnitude of the maximum resultant wave force is able to overcome the weight of the decks and the small, lateral resistance provided by the connections (Douglass et al. 2006).”

(b) Okeil, Ayman M., and C. S. Cai, "Survey of short-and medium-span bridge damage induced by Hurricane Katrina,” ASCE Journal of Bridge Engineering 13.4 (2008): 377-387:

> “Based on the observation of the writers, it may be concluded that storm-surge induced forces can easily overcome measures taken for anchoring existing bridges. This is due to the fact that bridge design is mainly controlled by gravity loads.”

(c) Padgett et al. "Bridge damage and repair costs from Hurricane Katrina." Journal of Bridge Engineering 13.1 (2008): 6-14:

"The most common severe failure mode for bridges was the unseating of individual spans. This failure often occurred in low elevation spans as a result of excessive longitudinal or transverse motion of the bridge deck. The deck displacement is attributed primarily to the severe storm surge, which led to a combination of buoyant forces and pounding by waves. Similarly, many bridge spans were shifted but did not experience a complete loss of support at the bents or abutments. Bearing damage typically accompanied span unseating or deck displacement. The bearings often provided no apparent positive connection between the superstructure and substructure. Some bridge spans, however, which were intended to have a fixed connection through doweling, still experienced complete loss of connectivity. Once the connectivity was lost, lateral wave and wind forces led to displacement of the bridge decks."

1.4 Problem Statement

GDOT can anticipate the hurricane vulnerability of its coastal bridge structures and economically prepare the state with a transportation infrastructure that is less susceptible to hurricane impact. Furthermore, this vulnerability assessment can contribute to the establishment of a Georgia Disaster Recovery and Redevelopment Plan (Georgia Office of Governor 2013). As these agencies have been tasked with identifying and quantifying the expected infrastructure, public health, economic, social and political consequences of future disaster events, it is critical for their success that they have a common understanding of the characteristics of hurricane hazards and how these events impact society at large.

Specifically for GDOT, it is extremely important to understand how these natural disasters will likely impact Georgia's transportation infrastructure network to include quantifying

the magnitude and extent of expected damage across the transportation system, predicting structural resilience for specific at-risk or mission critical bridges, estimating loss of system capacity through the network grid, and planning to mitigate infrastructure or operational vulnerabilities.

1.5 Objectives

The primary goal of this research study is to perform initial and secondary level analyses (Levels I and II) in accordance with the AASHTO Guide Specifications for Bridges Vulnerable to Coastal Storms (2008), hereafter referred as the 'AASHTO Guide', and to evaluate reliability of Georgia's coastal bridges under hurricane loads (e.g., wind, surge, and wave).

Specific objectives for this study include:

(1) Initial Screening of coastal bridges by comparing measured and predicted elevations;

(2) Level I Assessment by comparing self-weight of superstructures/bridge decks and vertical forces determined in accordance with the AASHTO Guide; and

(3) Level II Assessment by determining the probability of failure and its threshold for each coastal bridge comparing the vertical and horizontal forces computed by the AASHTO Guide and tensile and shear capacity of super-to-substructure connections, respectively, in addition to the capacity provided by the superstructure weight.

It should be recognized that the Level III assessment requires advanced numerical simulation of the sea state, shallow depth monitoring, and advanced determination of wave parameters (AASHTO 2008; Standford 2012) and is beyond the scope of this study.

1.6 Significance of Study

Through the research project, the Georgia Department of Transportation should be able to:

a. anticipate the hurricane vulnerability of its coastal bridge structures;
b. allocate available DOT resources for the most needed hurricane preparedness & recovery effort; and
c. prepare the state with a transportation infrastructure that is less susceptible to hurricane impact.

This study is not intended for providing retrofit strategies as the research findings are merely predictions of vulnerability, i.e., not absolute measures of bridge failure. Furthermore, it is focused on providing design recommendations, if applicable, for future coastal bridges and assisting GDOT with its recovery effort. This overall goal of the study is consistent with the objectives of the Moving Ahead for Process in the 21st Century Act (MAP-21). MAP-21 establishes a performance basis for maintaining and improving the National Highway System (NHS). States are required to develop a risk- and performance-based asset management plan for the NHS to improve or preserve asset condition and system performance. Under the asset management provisions enacted in MAP-21, codified at 23 U.S.C. 119, "state DOTs must develop and implement a risk-based Transportation Asset Management Plans," (FHWA 2012-2017). In addition to considering measures of bridge condition, GDOT may consider incorporating a risk factor associated with extreme events such as hurricanes for its coastal bridge asset management plans.

2. REVIEW OF AVAILABLE RESOURCES

2.1 The AASHTO Guide Specifications

The AASHTO Guide (2008) is utilized in this study. An important threshold for coastal bridges defined by this guide requires, "vertical clearances of highway bridges should be sufficient to provide at least 1 ft. of clearance over the 100-yr design crest elevation, which includes the design storm water elevation."

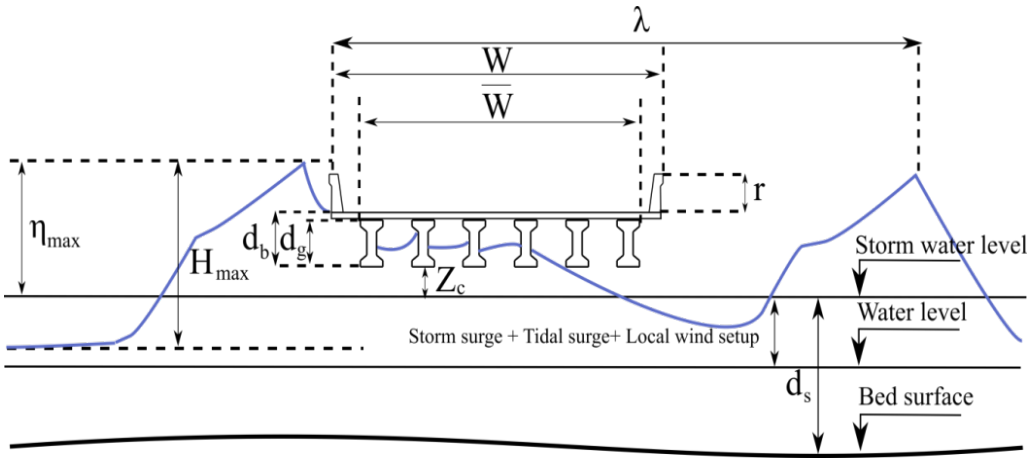

Figure 5 – Nomenclature Used in the AASHTO Guide.

Figure 5 shows the nomenclature used for defining wave parameters in order to determine wave forces. The major parameters used for the force calculations are listed below:

Water level = mean sea level (if storm surge includes astronomical tide)

d_b = bridge height (girder height + deck thickness)

d_g = girder height

d_s = storm water depth at the bridge

H_{max} = maximum wave height

Z_c = positive (or negative) distance from storm water level to bottom of the girder

η_{max} = wave crest height above storm water level

λ = wave length

r = rail height

W = deck width

W bar (or asterisk) = effective bridge width

The 100-year storm surge elevation is the increased mean water height of the body of water that will occur due to the occurrence of the 100-year design storm and is measured in reference to the North Vertical Datum. Therefore, determining the mean water depth of the body of water across the fetch length is critical. Fetch length is defined as the horizontal distance over water in which wind-generated waves are formed. The AASHTO Guide provides the basis for quantifying storm surge wave loading based on the wind speed and storm water level and for determining whether a coastal bridge is vulnerable or not.

In the AASHTO Guide (2008), three levels of analyses are recommended:

Level I: The simplest and generally most conservative of the three methods specified herein. Level I analysis is based on using relatively widely available information on wind speed, surge height, local wind set-up, astronomical tides, current speeds and information about the structure including bridge elevations, water depths, and fetch angle and lengths.

Level II: This approach uses best available hydraulic data usually determined through simulations of the sea state (e.g., SLOSH).

Level III *(beyond the scope of this study):* Advanced numerical simulation of the sea state is required, which usually starts with open sea modeling followed by shallow depth modeling and more advanced determination of wave parameters.

This study employs the Levels I and II procedures. The Level III analysis is beyond the scope of this study.

2.2 SLOSH MOM Model

The National Oceanic and Atmospheric Administration (NOAA) National Hurricane Center provides hurricane prediction models such as the Sea, Lake and Overland Surges from Hurricanes (SLOSH) model. 'SLOSH' is a computerized numerical model developed by the National Weather Service (NWS) to estimate storm surge heights resulting from historical, hypothetical, or predicted hurricanes by taking into account the atmospheric pressure, size, forward speed, and track data.

In this study, the SLOSH Maximum of Maximum (MOM) prediction model is used to display a Georgia's coastal region affected by the worst-case hurricane scenarios as shown in Fig. 6 and to identify coastal bridges that are potentially vulnerable to hurricanes. The region identified by the worst-case scenarios considers multiple hurricane tracks and the highest classification in the hurricane scale, Category 5, reserved for storms with winds exceeding 70 m/s (or 156 mph). Five hundred eighty six potentially vulnerable bridges (including 95 culverts) are identified in the coastal Georgia region, as illustrated in Fig. 6. The red 'cross' symbols, indicated by 'Surge Bridges' in Fig. 6, represent the locations of potentially surge-prone bridges.

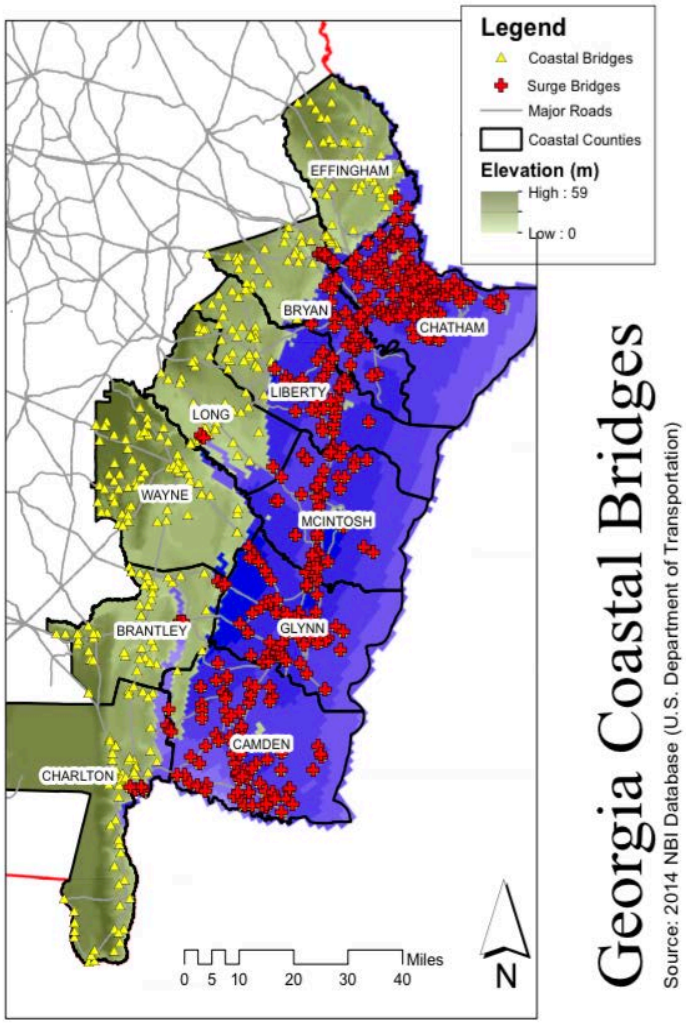

Figure 6 – 586 Potentially Surge-prone Bridges in the Coastal Georgia Region.

2.3 National Bridge Inventory Data

The National Bridge Inventory (NBI) database is used to meet several federal reporting requirements, as well as part of the states' needs (FHWA 1995). These requirements are set forth in the National Bridge Inspection Standards (23 CFR 650.3). By having a complete and thorough bridge inventory, an accurate report is made to the Congress on the number and state of the Nation's bridges (FHWA 1995). The NBI data is necessary for the Federal Highway

Administration (FHWA) and the Military Traffic Management Command to identify and classify the Strategic Highway Corridor Network and its connectors for defense purposes.

The primary purpose of utilizing the NBI database in this study is to identify the most commonly used bridge types, owners, year constructed, and other relevant information for Georgia's coastal bridges identified in Section 2.1. However, the NBI database is not intended to be solely used for the proposed hurricane vulnerability assessment, as it does not provide sufficient information to quantify the weight of the superstructure nor provides the super-to-substructure connection details necessary for evaluating the primary failure mechanism described in Section 1.3. Based on the NBI classification, approximately 83% of coastal bridges are simply supported as illustrated in Fig. 7. More than 66% of coastal bridges are made of concrete.

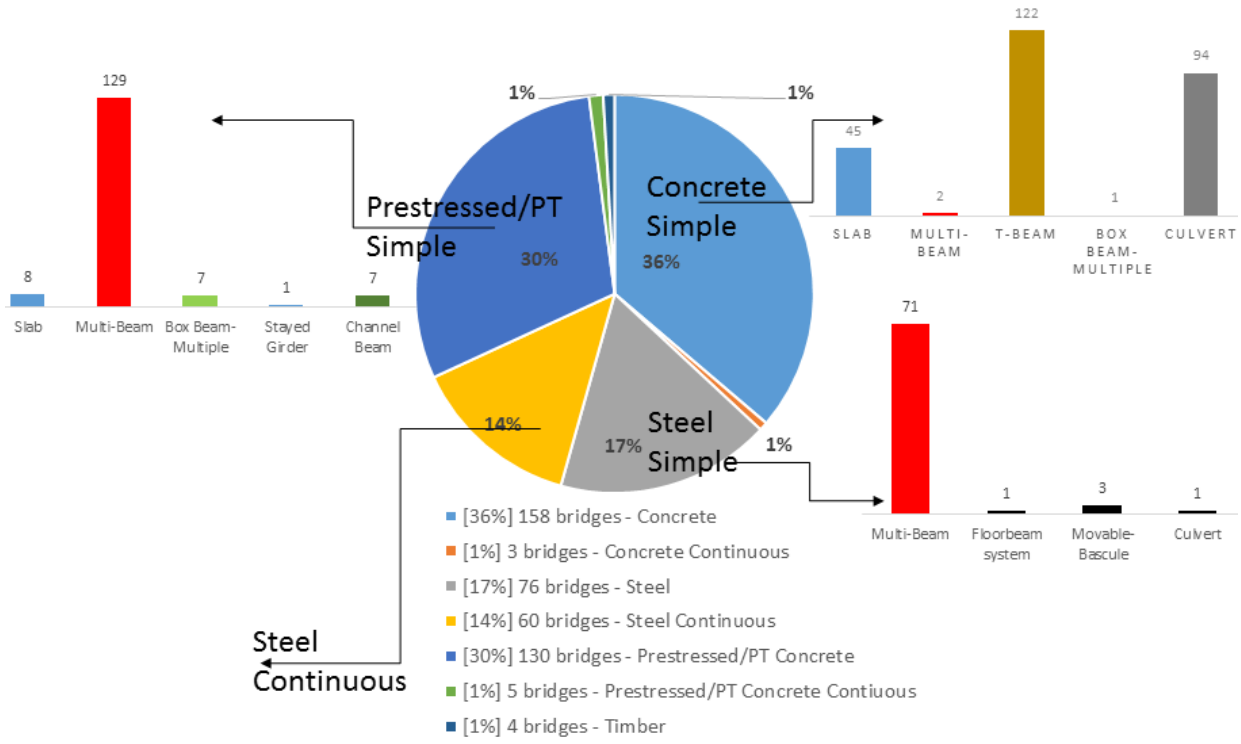

Figure 7 – Classification of Coastal Bridges.

2.4 Review of Available Bridge Drawings and Limitations

This section provides a brief explanation of bridge assessment components essential for the proposed vulnerability assessment. The weight of superstructure and tensile and shear capacity of bearing connections between super- and sub-structures must be determined by reviewing available bridge plans and drawings in the GDOT's bridge maintenance unit.

2.4.1 Superstructure Weight Calculations

The cross sectional area of superstructure is determined by reviewing available bridge drawings. The objective of this task is to determine the unit weight of bridge decks (including the top slab, girders, barriers, if available) per unit span length (kg/m or lb/ft).

2.4.2 Super-to-substructure Connection Types and Details

Elastomeric bearings are common in concrete bridges and transfer the bridge girder reactions to the substructure. The elastomeric bearing pads are generally attached to bridge substructures by means of either anchor bolts or dowels, as shown in Fig. 8. While dowels provide no vertical resistance against vertical uplift forces, anchor bolts retain bridge decks and carry vertical and horizontal wave loads from bridge superstructures into the substructures and thus provide additional vertical and shear resistance.

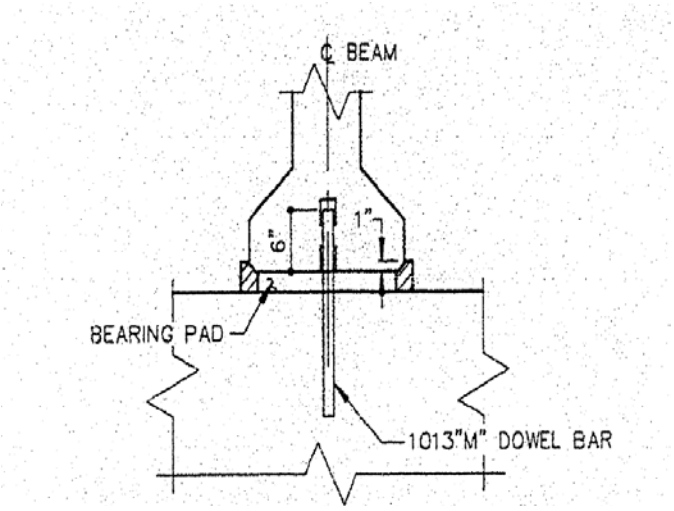

(a) Typical Dowel Connection

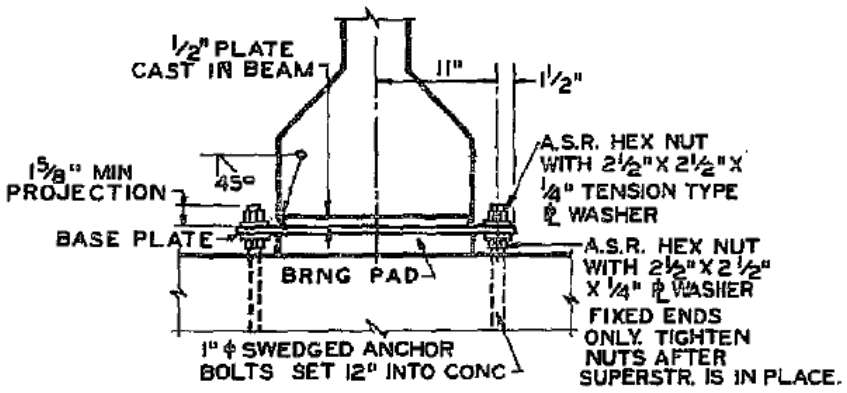

(b) Typical Anchor Bolt Connection

Figure 8 – Typical Bearing Connection Details.

(taken from available bridge drawings).

2.5 Review of BridgeWatch Program for Successful Implementation

This section provides a brief explanation of the BridgeWatch software GDOT subscribes to and its desired input parameters that will be determined through this study.

2.5.1 Description of BridgeWatch Software

BridgeWatch is a web-based monitoring software solution that enables bridge owners to predict, identify, prepare for, manage, and record potentially destructive environmental events (U.S. Engineering Solutions 2017). This software provides a hurricane module, in which bridge maintenance engineers are able to monitor bridge infrastructure in real time with the weather information provided by the National Hurricane Center to prioritize the recovery and inspection efforts during and after hurricanes.

2.5.2 Inputs Needed for BridgeWatch Software

It was identified during a web-meeting with the BridgeWatch team in September 2015 that the 'Bridgewatch' team desires that the following three questions be answered, in order to improve its hurricane module:

1. When does GDOT alert potential vulnerability? (i.e., threshold value)
2. When do bridge superstructures get wet?
3. When do bridge components fail (e.g., the threshold probability of failure measure)?

These three questions are addressed and/or answered by the study findings presented in Section 2.1, Section 4, and Section 6, respectively. Section 7 provides a summary of the findings.

2.6 Review of Fragility Analysis Models

The current state of research on the vulnerability assessment of bridges is presented in this section, leading to a literature review of fragility analysis models.

Literature Review

Fragility models provide a measure of structural reliability used to assess the vulnerability of different types of structures, including bridges, subjected to various hazards such as hurricanes and earthquakes. Reliability analysis methods generally provide necessary information for risk-based decision making considering all aleatory and epistemic uncertainties associated with structural response and hazard nature. The fragility analysis as a means of structural reliability assessment describes the probability of demand exceeding the capacity conditioned on a hazard intensity measure and other environmental parameters.

Fragility analysis of bridges subjected to various hazards has been extensively studied in recent years. In many instances, fragility estimates were used for seismic hazard (Guikema and Gardoni 2009; Karamlou and Bocchini 2015; Li et al. 2014). Nielson and DesRoches (2007) proposed a component-level approach for seismic fragility analysis of highway bridges in the central/southeastern regions of the United States. In their approach, the contribution of main bridge components such as columns and bearings to overall system fragility under earthquake events was investigated. Tavares et al. (2013) applied a similar method to generate fragility curves of highway bridges in Quebec for seismic events. Padgett and DesRoches (2008) expanded this method to generate fragility curves for seismically retrofitted bridges.

All aforementioned fragility analyses share a common feature. That is, the fragility is conditioned solely on hazard intensity measures. This type of fragility analysis can estimate how a certain class of bridges generally responds to different hazard intensity levels by presenting the

probability of damage. However in this approach, the probability of structural damage is not traditionally conditioned on bridge parameters.

Contrary to this traditional fragility analysis method, a parameterized fragility analysis model which estimates the probability of structural damage, *P*, conditioned on two vectors may be considered: an intensity measure vector (**IM**) and a bridge parameter vector (**X**) as shown in Eq. (1):

$$P[Demand > Capacity|\mathbf{IM}, \mathbf{X}] \quad (1)$$

The key to this parameterized fragility analysis lies in 'meta-models'. Meta-models, which are also referred to as surrogate models, are statistical methods which can predict the outcome of another model without making future inquiries to the original model. Meta-models predict failure of a specific bridge under various hurricane events. Once a surrogate is trained using a sample dataset, it is able to predict the performance of any bridge provided that the bridge parameters are within the range of the sample dataset.

Simpson et al. (2001) studied different meta-modeling techniques and their applications for various engineering problems. The application of meta-models in reliability analysis of structures has recently gained significant attention in earthquake engineering. Towashiraporn (2004) implemented meta-modeling techniques for a seismic fragility analysis of unreinforced masonry buildings. Ghosh (2013) performed a reliability assessment of aging highway bridges for seismic hazards using meta-models.

Application of fragility analysis is not limited to seismic hazard (Gernay et al. 2016). Ataei and Padgett (2012) conducted a fragility analysis of coastal bridges for hurricane-induced surge and wave forces. In their study, the distance from storm water level to the bottom of girder (Z_c) and maximum wave height (H_{max}) were used as hazard intensity measures. In a subsequent

study, Kameshwar and Padgett (2014) presented a risk assessment method for highway bridges under multiple natural hazard events using meta-models.

2.7 Review of Probabilistic Description of Demand Variables

Sheppard and Marin (2009) conducted an extensive experimental study to characterize wave forces acting on a bridge superstructure and proposed semi-empirical equations for maximum vertical, horizontal and slamming components of these forces, in terms of surge, wave, and bridge parameters. The AASHTO guide (2008) recommends using these equations to calculate wave-induced forces on bridge superstructure. However, the method provided by this guide yields an overly conservative estimation of wave forces because it deterministically provides wave parameters. On the other hand, the proposed risk assessment framework considers uncertainties in demand variables, surge height, extreme wave height, and wave period by deriving a joint probability of the two. The extreme wave height generally refers to the maximum wave height within a storm duration.

2.7.1 Probabilistic description of wave height

Short-term statistics of wave heights is considered. Longuet-Higgins (1975) proposed the Rayleigh distribution for the relative wave amplitude, ξ, as shown in Eq. (2). This method assumes a Gaussian process for sea surface elevation and a narrow-banded wave spectrum.

$$f(\xi) = \xi \exp(-\frac{\xi^2}{2}) \tag{2}$$

where $\xi = A/\sqrt{M_0}$, A is the wave amplitude defined as half the vertical distance between crest and trough; and M_0 is the 0^{th} moment of a wave spectrum. By virtue of the narrow-banded wave spectrum assumption, the wave height is considered twice the wave amplitude, $H \approx 2A$. By

replacing A with H/2 and rewriting Eq. (2) in terms of H and M_0, the Rayleigh distribution of wave height, H, is determined as follows:

$$f(H) = \frac{H}{4M_0}\exp(-\frac{H^2}{8M_0}) \quad (3)$$

Forristall (1978) used 116 hours of hurricane generated waves in the Gulf of Mexico to investigate the validity of Eq. (3) and concluded that the Rayleigh distribution "overpredicts the heights of the higher waves" in the record and proposed a two-parameter Weibull distribution for relative wave heights, $\widetilde{H}$, as shown in Eq. (4). This distribution provides a better fit for the wave data.

$$f(\widetilde{H}) = \frac{a}{b}\widetilde{H}^{a-1}\exp(-\frac{\widetilde{H}^a}{b}) \quad (4)$$

In which $a = 2.126$ and $b = 8.42$ are the distribution parameters empirically determined using the wave data; and $\widetilde{H} = H/\sqrt{M_{0,}}$. In a later study, Longuet-Higgins (1980) proposed a rescaled shape of the Rayleigh distribution or Eq. (3), which accounts for the width of the wave spectrum, and concluded that a modified Rayleigh distribution or Eq. (5) predicts the recorded wave height just as well as the Weibull distribution. The modification factor, α, is given by Eq. (5a) where ν is the spectrum bandwidth parameter determined by Eq. (5b).

$$f(H) = \frac{H}{4\alpha M_0}\exp(-\frac{H^2}{8\alpha^2 M_0}) \quad (5)$$

$$\alpha = \sqrt{1 - (\frac{1}{8\pi^2} - \frac{1}{2})\nu^2} \quad (5a)$$

$$\nu = \sqrt{M_0\, M_2/M_1^2 - 1} \quad (5b)$$

Several other studies examined the validity of these distributions, and some proceeded with proposed new formulations, which mostly are modifications of Eq. (3) or the Rayleigh distribution (Tayfun 1983; Casas-Prat and Holthuijsen 2010; Nayak and Panchang 2015). Casas-

Prat and Holthuijsen (2010) examined 10 million wave records measured by wave buoys in the Mediterranean Sea and compared them with various wave height distributions. They concluded that the Weibull distribution or Eq. (4) and modified Rayleigh distribution or Eq. (5) provide a much better agreement whereas the original Rayleigh distribution or Eq. (2) overpredicts recorded wave heights. In another study, Feng et al. (2014) investigated 10 years of wave measurements from Norwegian sea and reconfirmed that the Weibull distribution yielded better results than the original Rayleigh distribution in predicting H_{max}/H_s and H_{max}, noting that H_s is the significant wave height and H_{max} is the maximum wave height). A recent study by Nayak and Panchang (2015) also concluded that the original Rayleigh distribution (or Eq. 2) overestimates various quantities associate with wave height, and that the Weibull distribution provides a better fit to the recorded data.

Theoretical formulations, developed for determining wave height and wave amplitude distributions in deep water, such as those presented by Longuet-Higgins (Eq. (2), (3) and (5)), assume a Gaussian distribution of the sea surface displacement. Therefore, they are only applicable for analysis of bridges located in deep waters. Many of vulnerable coastal bridge are located within hurricanes surge prone areas; however, a majority of the bridges are not even on a waterway under normal conditions.

It has shown that the Rayleigh distribution reasonably works well for the shallow water waves (Thomton and Guza 1983). One of the first distributions for shallow water waves was the modified Rayleigh distribution proposed by Glukhovsky (1961), which accounts for the effect of depth-limited wave breaking. In this study, the modified formulation or Eq. (6), which is proposed by Klopman (1996) is considered:

$$f(H) = \frac{-A\kappa}{H} \exp\left(-A\left(\frac{H}{H_{rms}}\right)^{\kappa}\right) \quad (6)$$

where H_{rms} is the rms wave height given by $H_{rms} = H_s/\sqrt{2}$; $A = \left[\Gamma\left(\frac{2}{\kappa}+1\right)\right]^{\kappa/2}$; Γ is Gamma function; and κ is defined by Eq. (7) and is a function of $H^* = H_{rms}/d_s$.

$$\kappa = \frac{2}{1-\beta H^*} \tag{7}$$

$\beta = 0.7$ is an empirical parameter obtained from laboratory test results.

This study is primarily concerned with coastal bridges located in shallow waters although a number of other studies also addressed the deep water wave height and amplitude distributions (Tayfun and Fedele 2007; Naess 1985). Probability distributions of wave height discussed in this section are summarized in Table 1.

2.7.2 Conditional probability distribution of wave period

Contrary to wave height distributions, limited information on distributions of wave periods is found in the literature. Longuet-Higgins (1983) proposed a joint distribution of relative wave amplitude and relative wave period and derived the conditional distribution of relative wave period by Eq. (8), in which ξ is relative wave amplitude given in Eq. (2); and η is the relative wave period defined by Eq. (9):

$$f(\eta|\xi) = \frac{\xi}{\sqrt{2\pi}}\exp(-\frac{\xi^2\eta^2}{2}) \tag{8}$$

$$\eta = \frac{T-\bar{T}}{\nu\bar{T}} \tag{9}$$

, where T is the wave period, defined as the time interval between successive zero up-crossings; $\bar{T}$ is the mean spectral wave period; and ν is the spectral bandwidth parameter determined by Eqs. (10) and (11), in which M_i is the ith moment of a wave spectrum.

$$\bar{T} = 2\pi\left(\frac{M_0}{M_1}\right), \tag{10}$$

$$\nu = \sqrt{\frac{M_2}{M_0}}\frac{\bar{T}}{2\pi} \tag{11}$$

As discussed in the last section, the assumptions made by Longuet-Higgins to derive statistical distributions of wave height and wave period are only true for deep water conditions and may not be applicable to shallow or transit water. In an attempt to address this issue, Le Mehaute (1986) proposed statistical properties of shallow water by linear transformation of deep water properties and concluded that wave period distribution in shallow water is not Gaussian. He proposed a modified form of Longuet-Higgins equation (Eq. 12) for conditional distribution of relative wave periods, which includes a shoaling coefficient term (K_s), given by:

$$f(\eta|\xi) = \frac{\xi}{\sqrt{2\pi}}\exp(-\frac{\xi^2\eta^2}{2K_s^2}) \tag{12}$$

in which ξ and η are defined in the previous section and K_s is:

$$K_s = 1/(\sqrt{1+\frac{2kd_s}{sinh2kd_s}}\sqrt{tanhkd_s}) \tag{13}$$

where k is the wave number ($= 2\pi/\lambda$) and d_s is the water depth.

It should be recognized that Eq. (12) is no longer Gaussian since K_s is a function of wave period. The AASHTO Guide suggests using Eq. (14) obtained from the Shore Protection Manual (1984), in order to determine the wave length (λ) in shallow waters:

$$\lambda = \frac{gT^2}{2\pi}\sqrt{\tanh(\frac{4\pi^2}{T^2}\frac{d_s}{g})} \tag{14}$$

By rewriting Eq. (12) in terms of H, Eq. (15) determines the conditional distribution of wave period (T) for a given a wave height (H). The probability distributions of wave period discussed in this section are summarized in Table 1.

$$f_H(T) = \frac{H}{2\nu\sqrt{2\pi M_0 \bar{T}}} \exp\left(-\frac{H^2(T-\bar{T})^2}{8\nu^2 M_0 K_S^2 \bar{T}^2}\right) \quad (15)$$

2.7.3 Probabilistic distribution of extreme waves

The joint probability distribution of wave height and period of any randomly selected wave in a given stationary sea state, $f(H,T)$, is determined by Eq. (16) in which $f(H)$ and $f(T|H)$ are the probability distribution functions of wave height and conditional probability distribution of wave period, respectively.

$$f(H,T) = f(H).f(T|H) \quad (16)$$

2.7.4 Wave Spectrum

Statistical properties of sea surface is correlated to its underlying energy spectrum. A brief description of wave spectrum concept, various formulations of wave spectrum available in the literature, and spectral parameters is provided in this section.

Characterization of sea waves as a stochastic process with spectral analysis was initially introduced in the 1970s and 1980s. It was estimated that, at any given time, the ocean surface is determined as the result of superposed waves of different heights and periods. The total wave energy is unevenly spread among multiple waves exhibiting different characteristics. An ocean wave spectrum represents a distribution of wave energy for varying periods. Several idealized formulations for wave spectrum have been developed in the literature. Most wave spectra are

expressed by a standard exponential decay equation in terms of the wave angular frequency as shown in Eq. (17):

$$S(\omega) = \frac{C_1}{\omega^5} \exp(-\frac{C_2}{\omega^4} \quad (17)$$

S: Wave spectral density

ω: Wave angular frequency

C_1, C_2: Constants

One of the first wave spectra studied in the literature is the Pierson-Moskowitz (P-M) spectrum which was based on extensive measurements in the North Atlantic Ocean and is a function of $U_{19.5}$ defined as the wind speed measure at a height of 19.5 meters (Pierson and Moskowitz 1964). This spectrum was originally developed under the fully developed sea assumption (i.e., the wave crest phase speed equals the wind speed). However, Hasselmann et al. (1976) derived the same spectrum without fully developed sea assumption. A modified form of P-M spectrum with two parameters, namely Bretschneider Spectrum (B-S), was later developed and is widely used today since it does not require fully developed sea condition. The B-S spectrum expressed in terms of the angular frequency, ω, is as follows:

$$S_{B-S}(\omega) = \frac{5}{16} H_s^2 \omega_p^4 \omega^{-5} \exp(-\frac{5}{4}\left(\frac{\omega}{\omega_p}\right)^{-4}) \quad (18)$$

in which ω_p is the peak angular spectral frequency defined by the T_p is the peak spectral period, $\omega_p = 2\pi/T_p$.

In another significant international study, "The Joint North Sea Wave Observation Project (JONSWAP)" was carried out which collected wave data from 13 stations in the North

Sea, in order to investigate the waves developed in a "fetch-limited situation". Hasselman et al. (1973) proposed a new spectrum after analyzing the recorded data obtained from the JONSWAP, which was referred to as 'the JONSWAP spectrum' (Hasselmann et al. 1973). While JONSWAP is widely used by the offshore industry, further adjustments were proposed by other researchers to enhance the high frequency tail of the spectrum. While most wave spectra in the literature are formulated by an inversely proportional function of ω^{-5}, Battjes et al. (1987) demonstrated that estimating the wave spectrum in terms of ω^{-4} yields much better predictions in the high frequency band. This was later incorporated in the JONSWAP spectrum by Donelan et al. (1985), and Young made further amendments to represent the spectral parameters in terms of H_s and T_p. The modified form of the JONSWAP spectrum by Young or Eq. (19) is used for this study, and Equations (19a) through (19e) define the associated parameters.

$$S_{JONSWAP}(\omega) = \beta\, g^2 \omega_p^{-1} \omega^{-4} \exp\left(-\left(\frac{\omega}{\omega_p}\right)^{-4}\right) \gamma^{\delta} \tag{19}$$

$$\delta = \exp\left(-(\omega - \omega_p)^2 / 2\sigma_0^2\, \omega_p^2\right) \tag{19a}$$

$$\beta = 200 g^{-1.571} M_0^{0.786} T_p^{-3.143} \tag{19b}$$

$$\gamma = 6.489 + 6\log(2.649.10^7 g^{-2.857} M_0^{1.429} T_p^{-5.714}) \tag{19c}$$

$$\sigma_0 = 0.08 + 6.940.10^{-26} g^{8.571} M_0^{-4.287} T_p^{17.412}) \tag{19d}$$

$$M_0 = H_s^2/16. \tag{19e}$$

The JONSWAP spectrum was formulated using the similarity-law for deep water, which states that the shape of growing wind-generated wave spectra in deep water is reasonably consistent and thus can be described by a self-similar equation. Therefore, this spectrum may not be directly applicable for fragility assessment of coastal bridges in shallow waters. Bouws et al.

(1985) recognized that the wave number expression of the similarity-law can be developed for shallow water and proposed a frequency-depth dependency factor, $\phi(\omega, d_s)$, which transforms the JONSWAP spectrum developed for deep water into a spectrum for shallow water. They named the spectrum 'TMA' and successfully tested the spectrum with three available data sets (Battjes et al. 1987). The 'TMA' spectrum is described by Eq. (20), in which d_s is the water depth and the transformation formula for $\phi(\omega, d_s)$ is given by Eq. (21).

$$S_{TMA}(\omega, ds) = S_{JONSWAP}(\omega)\phi(\omega, d_s) \tag{20}$$

$$\phi(\omega, d_s) = \frac{k^{-3}(\omega, d_s)\frac{\partial k(\omega, d_s)}{\partial \omega}}{k^{-3}(\omega, \infty)\frac{\partial k(\omega, \infty)}{\partial \omega}} \tag{21}$$

In Eq. (21), the wave number, κ, is defined by $2\pi/\lambda$, where λ is the wave length. A simplified expression for Eq. (22) was proposed by Thomson and Vincent to determine ϕ in terms of ω_h, where $\omega_h = \omega\sqrt{d_s/g}$ and g is the gravitational constant.

$$\phi(\omega, d_s) = \begin{cases} {}^1\!/_2\,\omega_h^2 & \omega_h \leq 1 \\ 1 - {}^1\!/_2\,(2 - \omega_h)^2 & \omega_h > 1 \end{cases} \tag{22}$$

Ochi and Hubble (1977) proposed a new wave spectrum which accounts for both wind and swell. Waves generated by wind are the most common; however, wind is not the only mechanism by which ocean waves are created. In fact, waves generated at a specific point are the results of a superposition of several waves. Hurricane-generated swell (or ocean surface waves) is a good example. Swell refers to the waves generated by distant storms which generally have longer periods than wind generated waves (or dynamic of marine craft). After statistical analysis of 800 wave spectra obtained from North Atlantic Ocean, Ochi and Hubble developed a

family of spectra, each of which is the result of a superposition of a high frequency wind generated spectrum and a low frequency swell spectrum. This family of 11 spectra includes the most probable spectrum expected to occur for a particular sea state (i.e., significant wave height) and upper and lower bound spectral shapes, which are probable to occur with a 95% confidence coefficient of 0.95. Each of 11 Ochi-Hubble (O-H) spectra is formulated by Eq. (23) and uses unique coefficients (λ, ω) obtained by variables *a* and *b* shown in Eq. (24).

$$S_{O-H}(\omega) = \frac{1}{4}\sum_{j=1}^{2}\left(\frac{4\lambda_j+1}{4}\,\omega_{0j}^{4}\right)^{\lambda_j}\frac{1}{\Gamma(\lambda_j)}\frac{H_{sj}^{2}}{\omega^{4\lambda_j+1}}\exp\left(-\frac{4\lambda_j+1}{4}\left(\frac{\omega_{0j}}{\omega}\right)^{4}\right) \quad (23)$$

$$\omega_{01}, \omega_{02}, \lambda_1, \lambda_2 = aexp(-bH_s) \quad (24)$$

Base on a comparison of the four wave spectrum models, it is concluded that the TMA model is more accurate in shallow waters, whereas the other models work well for deep waters, and thus should be used in this study to estimate wave spectral parameters needed for calculation of wave height and period probabilities.

3. IDENTIFICATION OF ASSESSMENT PARAMETERS

The most important step for a vulnerability assessment involves the identification of bridge modeling parameters, including hydraulic data, from available GDOT database, GIS data, National Bridge Inventory (NBI), bridge drawings, and parameters in the AASHTO guide (2008). The most significant bridge modeling parameters are determined based on past hurricane studies (Padgett, 2009 and Ataei, 2010) and a sensitivity analysis of identified parameters.

3.1 Bridge Modeling Parameters

Critical bridge parameters are identified in, but not limited to, Table 1 to conduct a nonlinear analysis of bridges using the OpenSees (Mazzoni et al. 2006) analysis program.

Table 1 – Hurricane Category and Wind Speed.

Variables
Deck width
Number of spans
Spans length
Bridge height
Shear modulus of elastomeric bearing pad
Concrete strength
Steel strength
Entrapped air
Pile diameter
Deck weight variation
Dowel or anchor connection type
Dowel/anchor size
Dowel/anchor embedment length
Slab height

3.2 Environmental Parameters

Two most significant environmental parameters are investigated. The first parameter is the storm water depth at each bridge location, d_s, shown in Fig. 5. The storm water elevation is directly affected by storm surge elevation as well as the wave height and period, which in turn is affected by the wind speed. The second parameter is the wind speed. The Saffir–Simpson scale for categorizing hurricane intensity is associated with wind speeds (e.g., peak 1-minute wind speed).

3.2.1 Best Available Hydraulic Data

The AASHTO Guide (2008) suggests that the design water level should be based on more realistic hydraulic data obtained from public agency repositories. The study team investigated best publically available hydraulic data. The FEMA Region IV's Atlantic coastal floodmap data was considered; however, the latest SLOSH data published in 2014 is selected. It should be recognized that the SLOSH prediction models are one of available hydraulic data selected for this study because it is more suitable for data extraction and analysis needed in this study.

A Flood Insurance Rate Map (FIRM) produced by FEMA and the Hurricane Inundation/Evacuation Maps produced by the National Oceanic and Atmospheric Administration's (NOAA) are fundamentally different. The NOAA's Hurricane Inundation/Evacuation maps depict areas that are subject to hurricane surge inundation for established storm intensities (usually on the Saffir-Simpson scale). The FIRMs represent the areas subject to inundation by the 1-percent-annual-chance flooding and the water surface elevations having a 1-percent-annual-chance of exceedance. There are also differences between the two models and the underlying methodologies. For example, NOAA's maps do not incorporate wave effects while FIRMs do. Therefore, it is difficult to compare the Base Flood Elevations (BFEs) and water elevations produced by NOAA's SLOSH (Sea Lake and Overland Surges from Hurricanes) model.

3.2.2 Wind Speed

The design wind velocity at the standard 9.8 meter (32.2-ft) elevation and averaged for a duration of 10 minutes (m/s or ft/s), U_{10min}, where $U_{10min} = 0.7\ U_{3sec}$. The ASCE standard 7

tabulates winds for a 50-year event based on a 3-second gust, and therefore the ASCE 7 provides a conversion factor of 1.07 for the continental U.S., in order to determine the 100-year coastal storm wind speed.

The Hurricane Center uses a 1-min averaging time for reporting the sustained (i.e. relatively long-lasting) winds. The Saffir-Simpson Hurricane Wind Scale is a 1 to 5 rating based on a hurricane's sustained wind speed (NOAA 2017). This scale estimates potential property damage. Hurricanes reaching Category 3 and higher are considered major hurricanes because of their potential for significant loss of life and damage. Category 1 and 2 storms could still be dangerous; however, they require preventative measures (NOAA 2017).

Table 2 – Hurricane Category and Wind Speed (1-minute wind speed).

Category	NOAA-Sustained Winds
1	74-95 mph (119-153 km/h)
2	96-110 mph (154-177 km/h)
3	111-129 mph (178-208 km/h)
4	130-156 mph (209-251 km/h)
5	> 157 mph (252 km/h or higher)

Based on a logarithmic-law model, depending upon assumptions pertaining to the surface roughness for flow over open water and an estimation method, the ratio of 1-min speeds to peak 3-second wind speeds range between 1.03 and 1.12 (Simiu et al. 2007). For structural engineering purposes, the 3-second wind speed may be determined by 1.43 U_{10min} (Simiu et al. 2007), which is consistent with the 0.7 factor used in the AASHTO Guide (U_{10min} = 0.7 U_{3sec}). For risk assessment (Section 6.4), the sustained wind speed (i.e., the 1-minute wind speed) and annual rate of exceedance are determined by means of a hazard curve. More details are presented in Section 6.4.

3.2.3 Environmental parameters

The level of uncertainty in a fragility model is highly dependent on hazard intensity measures (IMs) selected for analysis (Padgett et al. 2008). A suitable IM is directly correlated with the level of demand exerted on a bridge while it is a measure of hazard intensity. The sensitivity study presented in this sub-section utilizes two IMs, U_{10min} and d_s, to generate a fragility model. U_{10min} is selected because the sustained wind speed is a measure used for hurricane categories on the Saffir-Simpson Wind scale (Simpson and Saffir 1974), thus an acceptable measure of hurricane intensity. While the wind speed is directly related to wind wave heights and forces, it cannot represent the magnitude of wave forces applied to the bridge deck by itself as bridges with greater freeboard height are less prone to wave forces. Therefore, it is necessary to consider d_s as the second IM.

Finally, the research team has enabled a risk assessment of coastal bridges (Sections 6.3 and 6.4) in terms of a single hazard intensity parameter. The hazard IM is the sustained wind speed, which is consistent with the Saffir-Simpson Hurricane Wind Scale, by means of using a wave spectrum and a joint probability of wave period and height. More details are presented in Section 6.4.

3.2.4 Wave Induced Forces

Equations (2) through (4), shown below, are provided in the AASHTO Guide (2008) and are the result of extensive studies conducted by Sheppard (2008). Wave forces include the contribution of both hydrostatic and hydrodynamic forces. The vertical wave force comprises of a low-frequency quasi-static mechanism and a short-duration, high-frequency slamming force. The

vertical quasi-static wave force, $F_{V\text{-}Max}$, includes the effect of buoyancy force, drag force, and inertia forces. To calculate wave forces, wave parameters (period, height, and length) are derived for each IM combination (d_s and wind speed) and are used to determine the maximum vertical/horizontal forces and overturning moments. Wave parameters for a given location are a function of wind speed, water depth, fetch length, and wind duration.

The maximum vertical quasi-static wave force per unit length of the deck, $F_{V\text{-}Max}$, is obtained by Eq. (25), where γ_w is the unit weight of water, $\bar{W}$ is the deck width factor, β is a function of wave crest height and distance between water level and deck low chord, H_{max} is the maximum wave height, d_s is the storm water elevation at the bridge location, T_P is the wave period, $x = H_{max}/\lambda$, $y = \bar{W}/\lambda$, and λ is the wavelength. Parameters b_0-b_6 and *TAF* (Trapped Air Factor) are related to the effect of trapped air between water surface and voids beneath bridge girders.

$$F_{V-Max} = \gamma_w \bar{W} \beta (-1.3 \frac{H_{max}}{d_s} + 1.8)(1.35 + 0.35 \tanh(1.2\, T_p - 8.5))(b_0 + b_1 x + \frac{b_2}{y} + b_3 x^2 + \frac{b_4}{y^2} + \frac{b_5 x}{y} + b_6 x^3)(TAF) \quad (25)$$

The maximum horizontal force per unit length of the deck, $F_{H\text{-}Max}$, is determined by Eq. (26), where ω is defined by Eq. (26-a), in which η_{max} is the wave crest height above storm water, d_b is the deck height, r is the rail height, and W is the deck width. The vertical slamming force, F_s, per unit length of the deck is determined by Eq. (27), where A, B are two factors which are determined as a functions of Z_c/η_{max}.

$$F_{H-Max} = F^{*}_{H-Max} \exp(-3.18 + 3.76 \exp\left(\frac{-\omega}{\lambda}\right) - 0.95 \left(\ln(\frac{\eta_{max}-Z_c}{d_b+r})\right)^2) \quad (26)$$

$$\omega = \min\left(\lambda - {}^{1}/_{2}\left(Z_c + {}^{1}/_{2}\, H_{max}\right)\left(\frac{\lambda}{H_{max}}\right), W\right) \quad (26\text{-a})$$

$$F_s = A\, \gamma_w H^2_{max} \left(\frac{H_{max}}{\lambda}\right)^B \quad (27)$$

These vertical and horizontal forces represent possible peak values, and the AASHTO Guide does not explicitly describe how these forces should be applied to the bridge structures or components. No detailed discussion of a wave load-time history that may be exerted on a bridge is available in the AASHTO Guide. Therefore, this study adopts the method suggested by Ataei (2013) to generate a time history function for waves forces. Quasi-static components of wave forces in both vertical and horizontal directions are considered to be in phase with wave and vertical slamming forces.

Figure 9 depicts a variation of maximum values of vertical, slamming and horizontal components of wave force ($F_{V\text{-}Max}$, F_s or $F_{H\text{-}Max}$) versus variations of U_{10min} and d_s for a sample bridge computed in accordance of the AASHTO Guide. Z_c in Figs. 9 (a) and (b) denotes the distance between the storm water level and bottom of a bridge deck. A negative value indicates that the water elevation is above the height of bridge low chord. In both cases ($Z_c > 0$ and $Z_c < 0$), Figs. 9(a) and (b) show that the vertical force components ($F_{V\text{-}Max}$, F_s) generally increase as the wind speed increases, although a slight decrease is observed between Categories 4 and 5 (indicated as 'CAT' 4 and 5 in the figure). The horizontal force component does not necessarily increase with increasing wind speed. Figs. 9(c) and (d) depict a variation of wave forces as the

storm water elevation changes. A significant correlation is observed between the quasi-static component ($F_{V\text{-}Max}$) and storm water elevation (d_s).

There are other interesting trends observed from Fig. 9. To better investigate the effect of the variables on the vertical wave force, $F_{V\text{-}Max}$, shown in Eq. (25), Fig. 10 presents the variables as a function of U_{10min} and d_s. As stated above, the vertical force ($F_{V\text{-}Max}$) increases until the threshold wind speed for *CAT 4* hurricane is reached and remains constant. However, it slightly decreases through categories 4 and 5. While the magnitude of $F_{V\text{-}Max}$ is dependent on various terms, the trend is mainly attributed to the terms including the effect of wave period (T_P) as shown in Fig. 10(d).

While the vertical force ($F_{V\text{-}Max}$) is generally greater when a bridge is submerged ($Z_c < 0$), provided the wind speed remains constant, the slamming force component is much smaller and thus is considered insignificant. This can be explained by the fact that the quasi-static component is mainly governed by hydrostatic forces and thus is greater when a bridge is submerged. On the other hand, slamming forces decrease because there is no air trapped between water surface and bridge deck once the bridge is submerged. As shown in Fig. 10(a), the term representing the effect of wavelength ($\overline{W}$) increases with growing wind speed. This is due to the fact that waves generated by stronger winds have greater wavelengths. This consequently results in a wider bridge area affected by waves.

Fig. 10(b) shows a variation of the term β which represents the effect of hydrostatic forces. As expected, 'b' increases with increasing wind speed because a greater portion of bridge deck submerges as the wave height increases. As presented in Figs. 9 (c) and (d), the slamming force component in both cases is increased to the point where a snap-through occurs, and slamming forces is reduced beyond this point. This is the point where the bridge is

submerged, and trapped air pockets are fully vented. As shown in Fig. 10(a), $\overline{W}$ increases as the water elevation rises for a constant wind speed. Figure 10(b) illustrates the importance of considering sufficient freeboard height as ‘b’ increases due to rising water elevation.

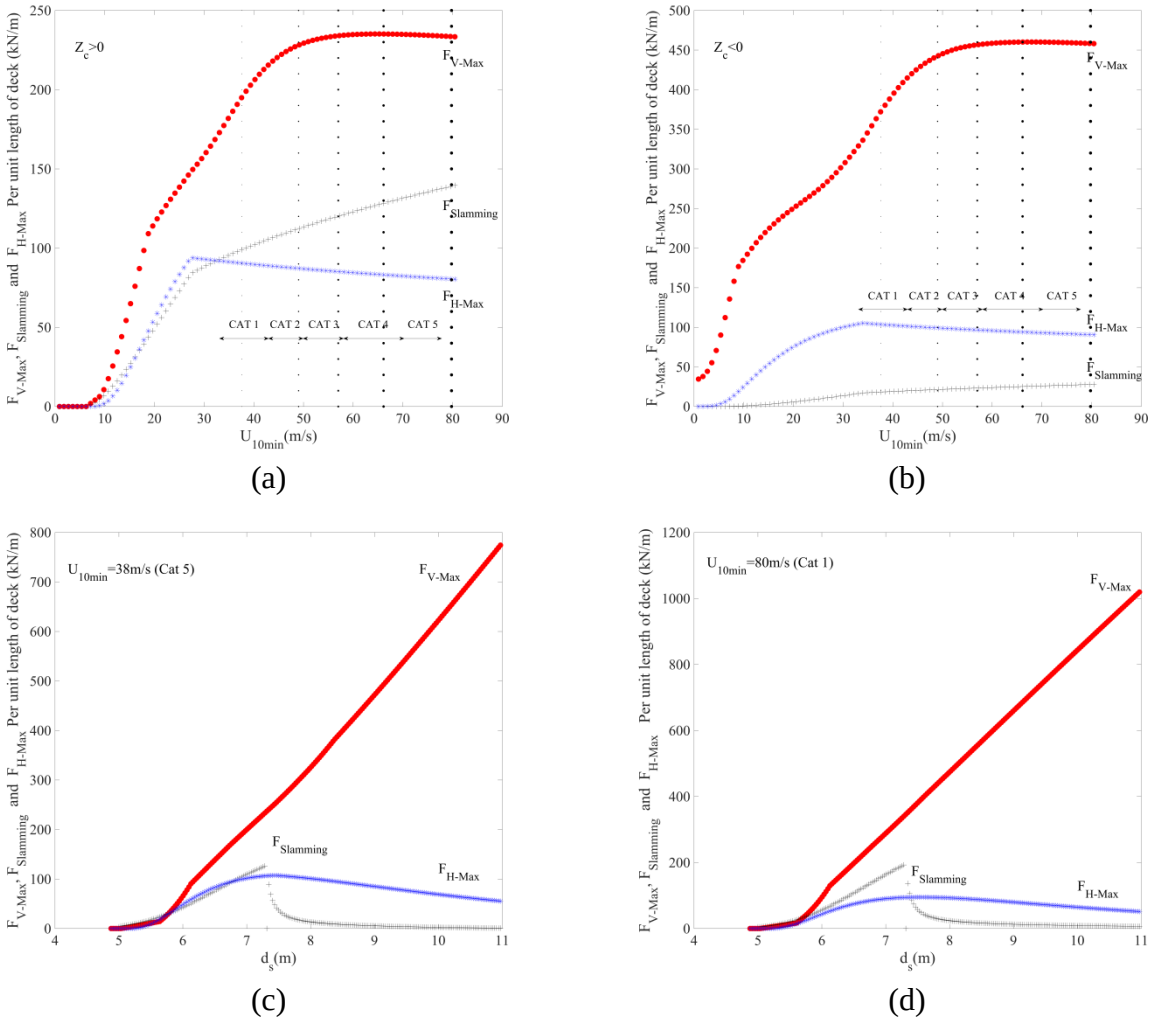

Figure 9 – Vertical and Slamming Forces In Terms of Intensity Measures.

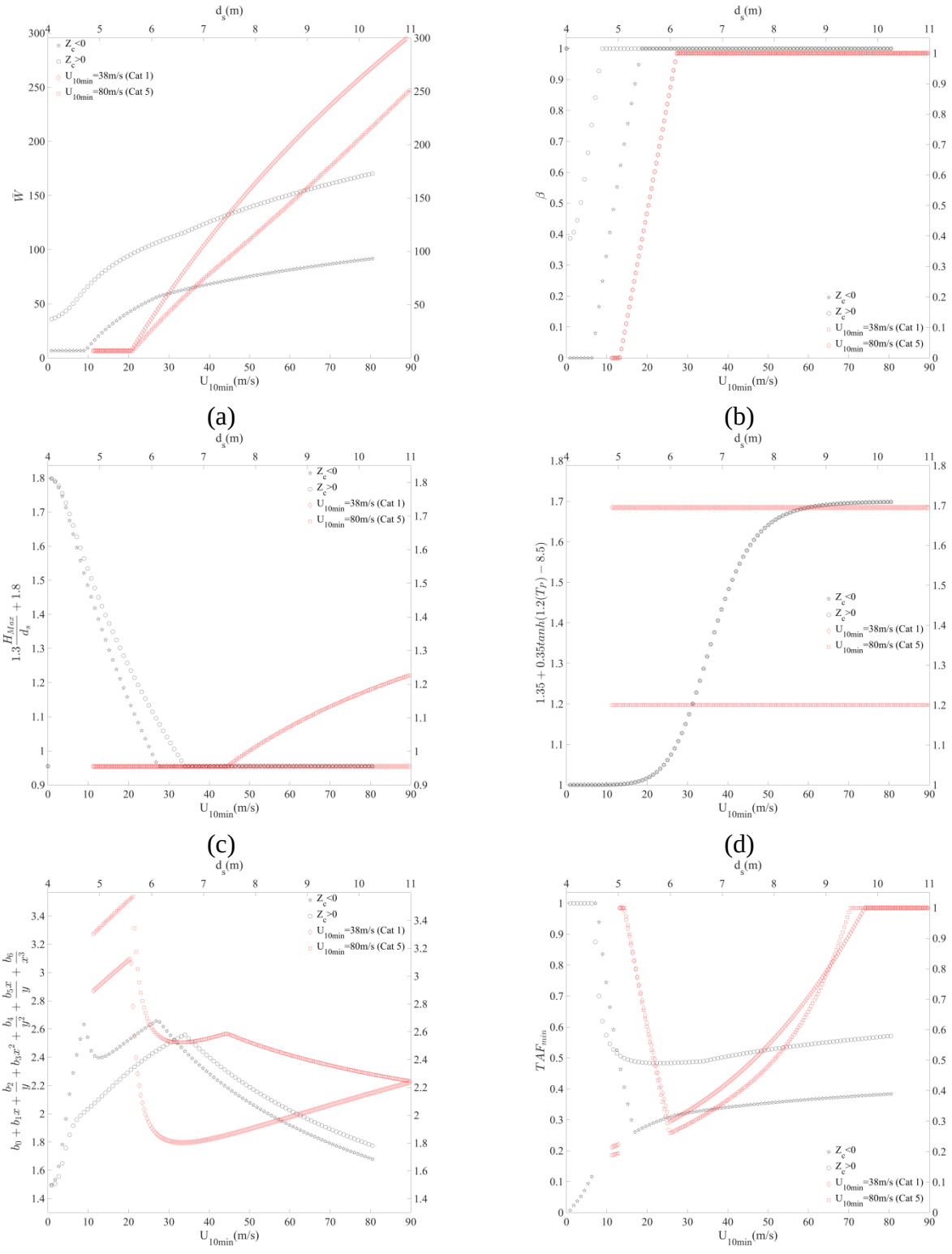

Figure 10 – Wave Parameters in Terms of Intensity Measures.

4. INITIAL SCREENING

Using expected flood surge/tide levels and wind-wave heights for each category event from the SLOSH MOM model, the initial screening compares as-built bridge deck surface elevations with the calculated water surface elevations to determine if the bridge deck is likely to be inundated. The structures, which are submerged for Category 5 hurricanes using the high-tide storm water surface, are considered for further assessments.

4.1 Field Measurement of Bridge Deck Surface Elevations

The study team conducted a field investigation of the 586 coastal bridges identified in Section 2.1 and relevant bridge components. Fig. 11 illustrates a coastal bridge that is potentially vulnerable for hurricane-induced wave forces. The primary goal of this site visit is to accurately (i.e., the error <1 inch) measure the bridge elevation as shown in Fig. 12. The secondary goal of this site visit is to enhance the understanding of site conditions. Unfortunately, the bridges owned by the national parks and military/navy were not easily accessible with the surveying equipment and thus are not further pursued as a part of this study.

Figure 11 – Typical Coastal Bridge Potentially Vulnerable for Storm Surge/Wave Forces.

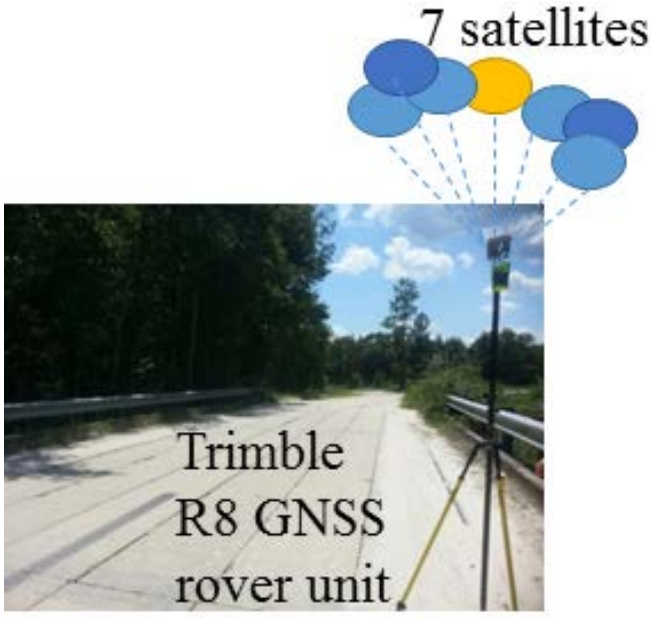

Figure 12 – Elevation Survey Using a Trimble R8 RNSS Unit.

4.2 Predicted Storm Surge Elevations by NOAA's SLOSH MOM

For each hurricane category, both mean and high tide storm water elevations are considered as shown in Fig. 13 and Fig. 14, respectively. This is also because the elevation difference between the bridge top surface and bottom of girders ranges between 0.61 m and 1.52 m (2 and 5 feet). Similar elevation difference exists between the mean-tide and high-tide storm water elevations, and thus in this initial screening, both high and mean-tide cases are considered. It is important to recognize that considering the high-tide case alone may result in overly conservative assessment of submerged bridges due to the fact that the elevation survey was conducted at the top surface of bridge decks. Figure 14(f) provides the median and quartiles of predicted storm surge elevations from the SLOSH MOM model.

(a) Category 1

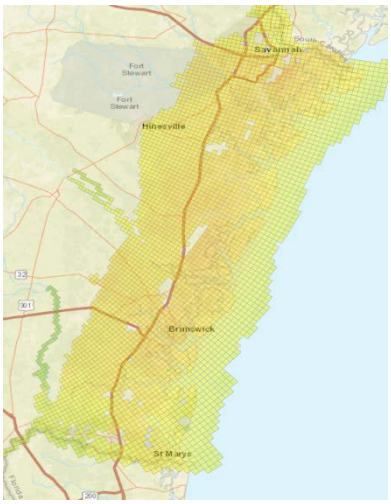

(d) Category 4

(b) Category 2

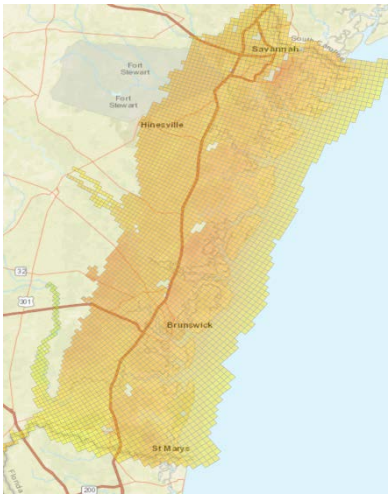

(e) Category 5

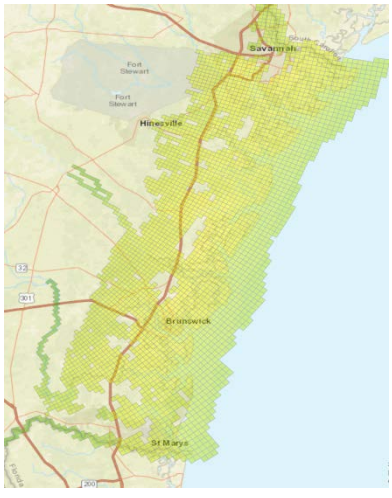

(c) Category 3

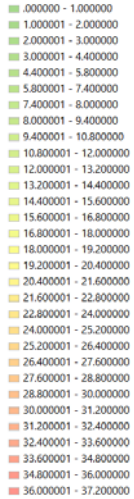

Scale (NAVD88): elevation, ft

Figure 13 – SLOSH Storm Water Elevations (Mean tide).

(a) Category 1

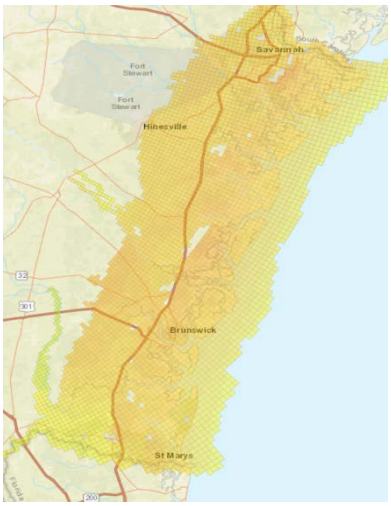

(d) Category 4

(b) Category 2

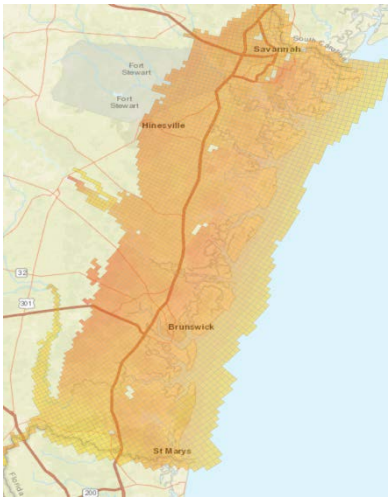

(e) Category 5

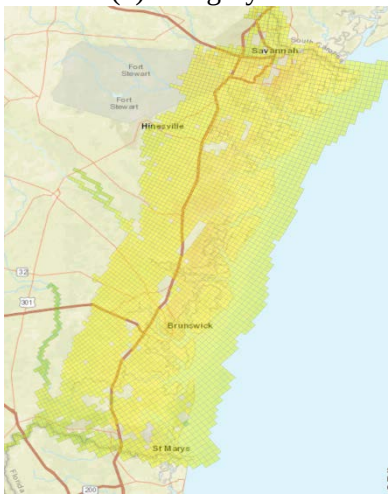

(c) Category 3

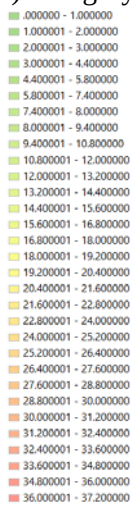

Scale (NAVD88): elevation, ft

Figure 14 – SLOSH Storm Water Elevations (High tide).

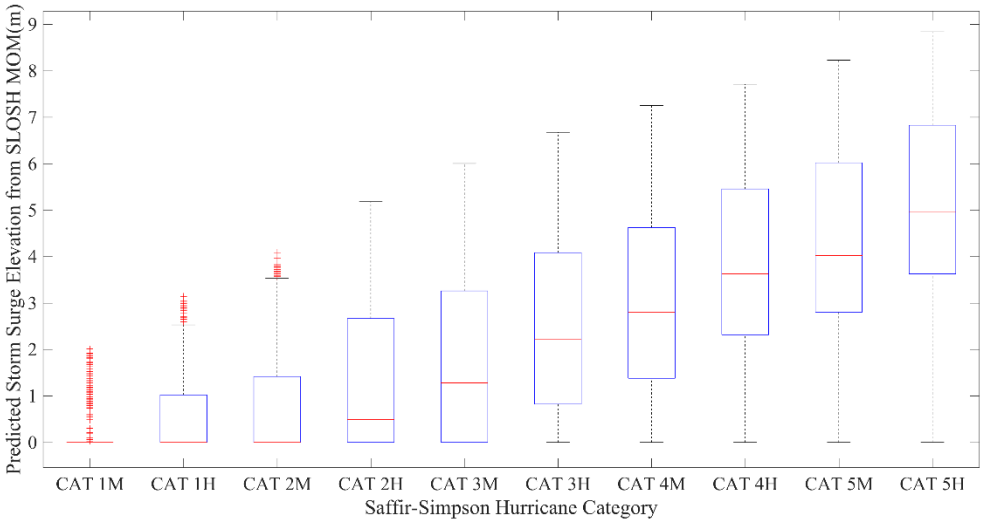

(f) Median and quartiles of predicted storm surge elevations from the SLOSH MOM model for Georgia coastal bridges (CAT: category; M: mean tide; H: high tide)

Figure 14 Continued – SLOSH Storm Water Elevations.

4.3 Comparison of Measured and Predicted Elevations

4.3.1 Results

It is anticipated during a most severe Category 3 hurricane event that 216 and 273 bridges are expected to be submerged based on the mean and high storm water levels considered, respectively, in this study. A visual comparison of the two cases with respect to the measured bridge elevations is shown in Figs. 15 and 16. Figure 17 presents a three-dimensional illustration of bridge elevations, indicated by the tips of red lines, and topology rendering with respect to the storm water elevations determined from the SLOSH model.

4.3.2 Summary and Discussion of the Results

During this initial screening, the highest storm water level was used to screen 353 (of 586 in Section 1.2) coastal bridges for further assessment (i.e., the AASHTO Level I/II assessment). The difference in the number of bridges using the mean and high storm water levels is 15 (bridges), which was considered relatively insignificant with respect to the 586 coastal bridges initially identified by the worst case hurricane scenario in Section 2.1. A comparison of the results due to the two storm water levels is shown in Table 3. Table 4 provides a summary of bridge counts by bridge owners. Table 5 provides the same summary of bridge counts, not including culverts.

It is concluded that the elevation survey accurately determines whether each bridge is submerged for each hurricane category. It is also concluded that bridges considered submerged by Category 5 is located in the surge-prone region identified in Fig. 6.

Table 3 – The Number of Bridges Considered Submerged for Each Category.

Hurricane Category	CAT 1	CAT 2	CAT 3	CAT 4	CAT 5
Count (Mean-tide)	0	66	216	302	338
Count (High-tide)	18	156	273	325	353

Table 4 – The Number of Bridges (Including Culverts) Submerged - by Owners.

Method of Evaluation	Owner	Number of submerged bridges				
		CAT 1	CAT 2	CAT 3	CAT 4	CAT 5
Initial Screening (High Tide)	State Highway Agency	7	88	164	204	228
	County Highway Agency	10	61	94	104	108
	City/Municipal Highway Agency	1	6	14	16	16
	State Park/Forest/Reservation	0	1	1	1	1
	Total	**18**	**156**	**273**	**325**	**353**

Table 5– The Number of Bridges (Not Including Culverts) Submerged - by Owners.

Method of Evaluation	Owner	Number of submerged bridges				
		CAT 1	CAT 2	CAT 3	CAT 4	CAT 5
Initial Screening (High Tide)	State Highway Agency	7	75	124	152	172
	County Highway Agency	9	49	71	74	77
	City/Municipal Highway Agency	1	5	11	12	12
	State Park/Forest/Reservation	0	1	1	1	1
	Total	**17**	**130**	**207**	**239**	**262**

(a) Category 1

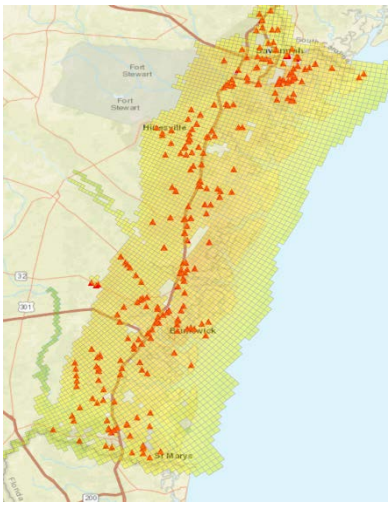

(d) Category 4

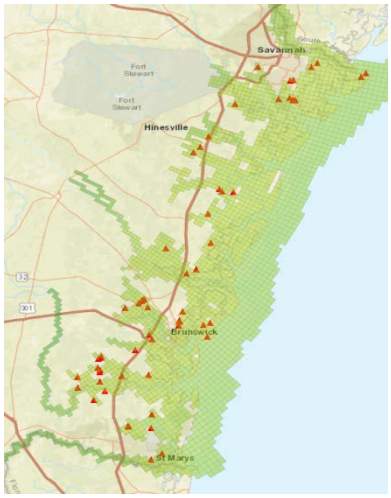

(b) Category 2

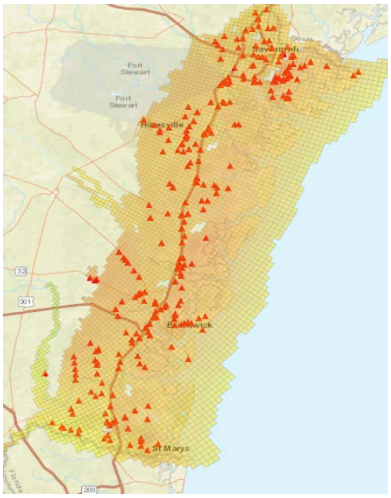

(e) Category 5

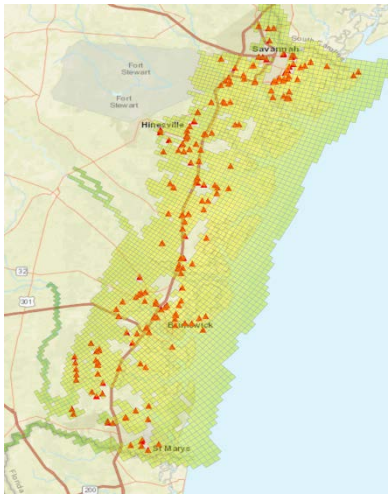

(c) Category 3

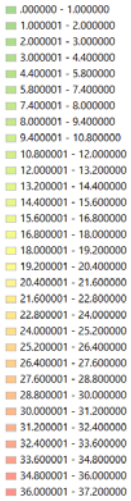

Scale (NAVD88): elevation, ft

Figure 15 – Submerged Bridges for High Storm Water Level (Mean-tide).

(a) Category 1

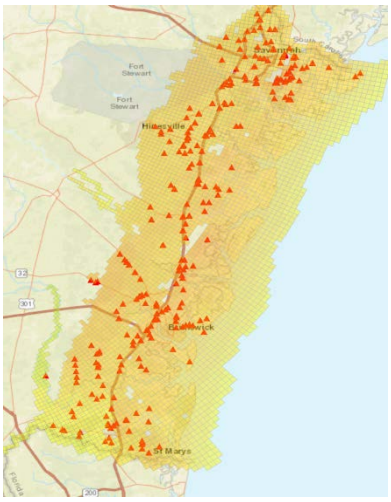

(d) Category 4

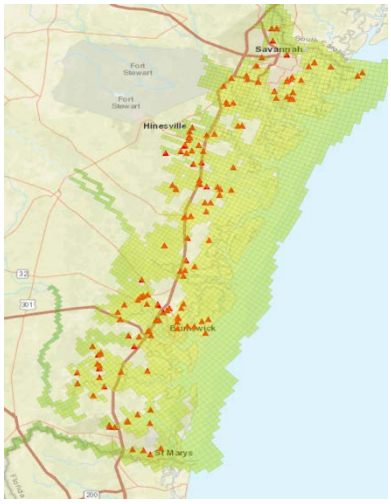

(b) Category 2

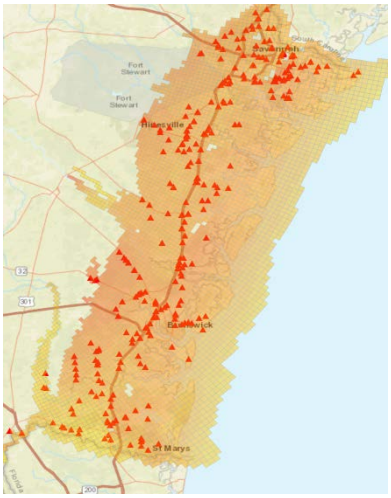

(e) Category 5

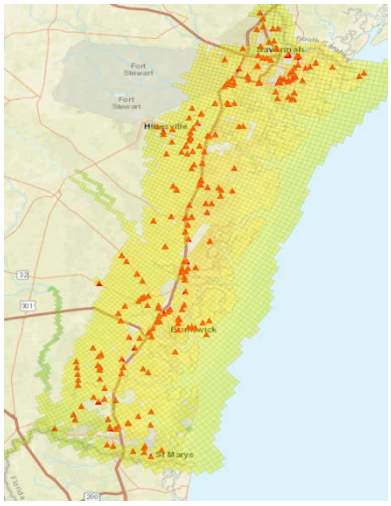

(c) Category 3

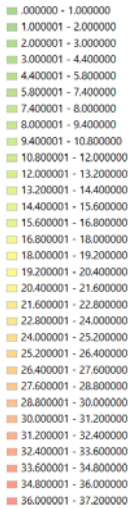

Scale (NAVD88): elevation, ft

Figure 16 – Submerged Bridges for High Storm Water Level (High-tide).

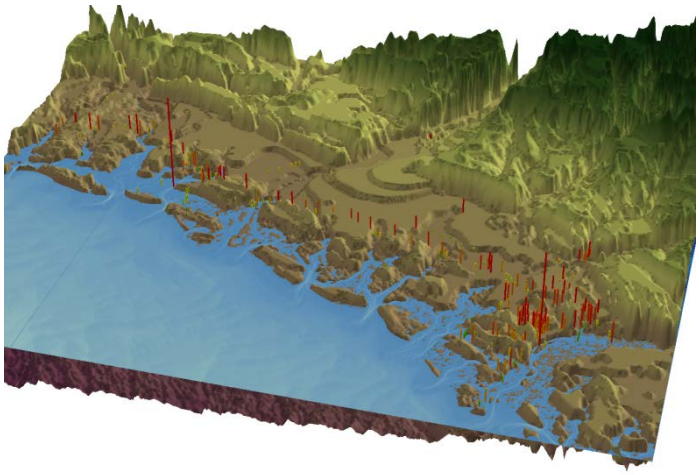

(a) Mean Low Water: The average of all the low water heights observed over the National Tidal Datum Epoch.

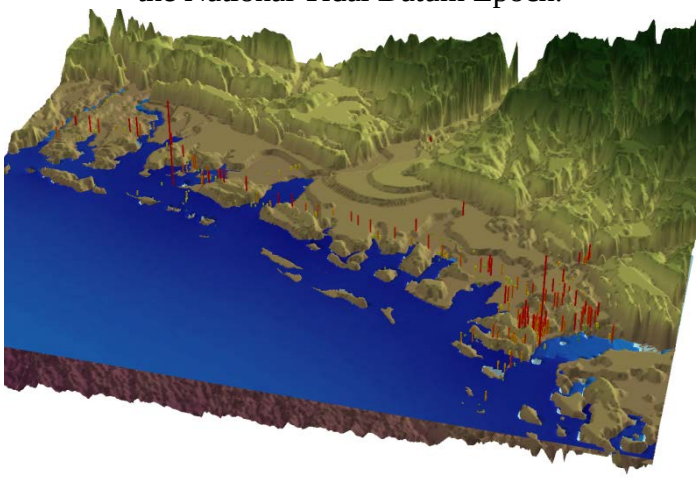

(b) Category 1

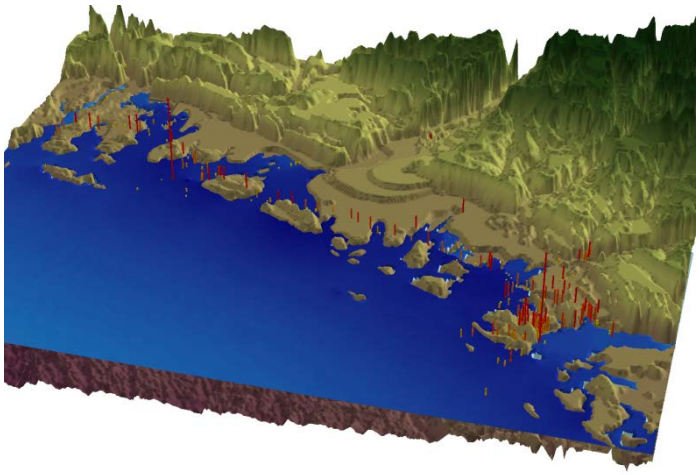

(c) Category 2

Figure 17– Bridge Elevations vs. SLOSH Storm water elevations using the ArcScene program.

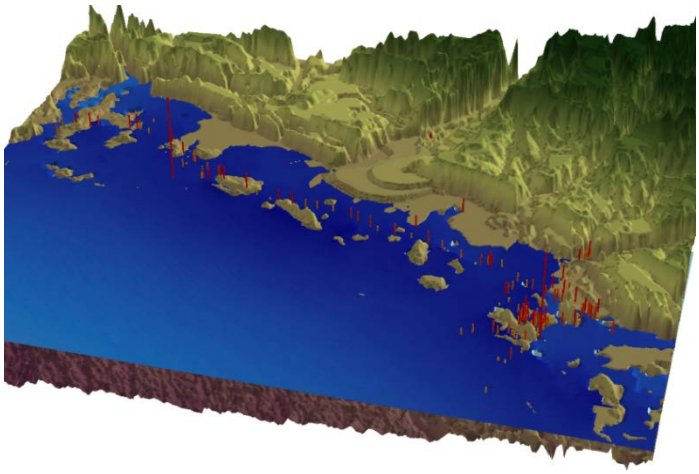

(d) Category 3

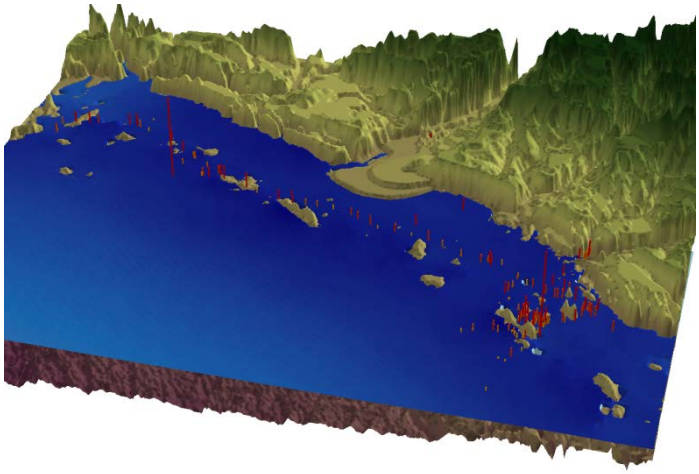

(e) Category 4

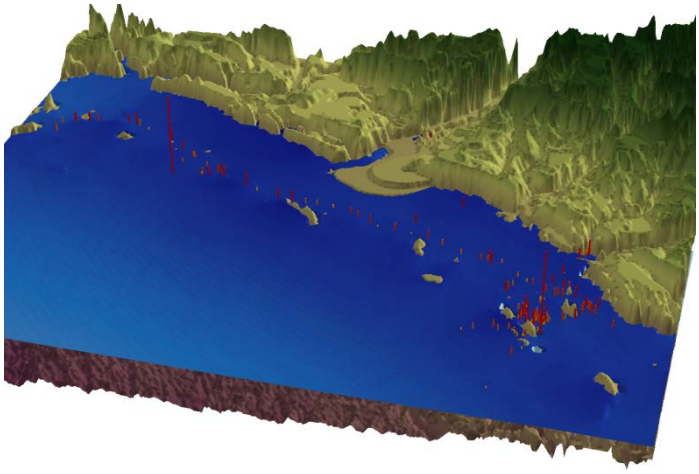

(f) Category 5

Figure 17 Continued– Bridge Elevations vs. SLOSH Storm water elevations using the ArcScene program. (Note): The top of the tips in the red line indicate bridge deck surface locations, and the blue color indicates the increasing sea level for each hurricane category).

5. LEVEL I ASSESSMENT

5.1 Methodology

For the coastal bridge structures forwarded from the initial screening, the Level I analysis is performed. Furthermore, the other bridges that were not submerged in Section 4 are reassessed in this section because bridges that are not submerged could fail by hurricane-induced wave loads. The AASHTO Guide (2008) states that the Level I assessment is the most conservative approach which relies on using relatively widely available information on wind speed, surge height, local wind set-up, astronomical tides, current speeds and information.

The Level I analysis considers the inundation potential of each structure to Category 1 through 5 events, and also provides structural loading analyses to determine if the forces generated are significant compared to each bridge's structural dead weight. The current NOAA SLOSH models are used to extract water surface elevations for five Hurricane Categories by bridge location.

The purpose of conducting the Level I analysis in this study is to identify bridges that were not designed to be held in place by the gravity load of their own self-weight. In conducting the Level I analysis, the vertical force, 'FV-total', shown in Fig. 18 is directly compared to the weight of superstructure. The eccentricity, 'e', due to the wave movement (or torsional load, 'Fe') is not considered in determining the vertical force in the Level-I analysis but will be included in the Level-II analysis. Furthermore, the lateral wave force being applied from the waves is not evaluated in comparison with the frictional resistance between the pier cap beams and bridge girders.

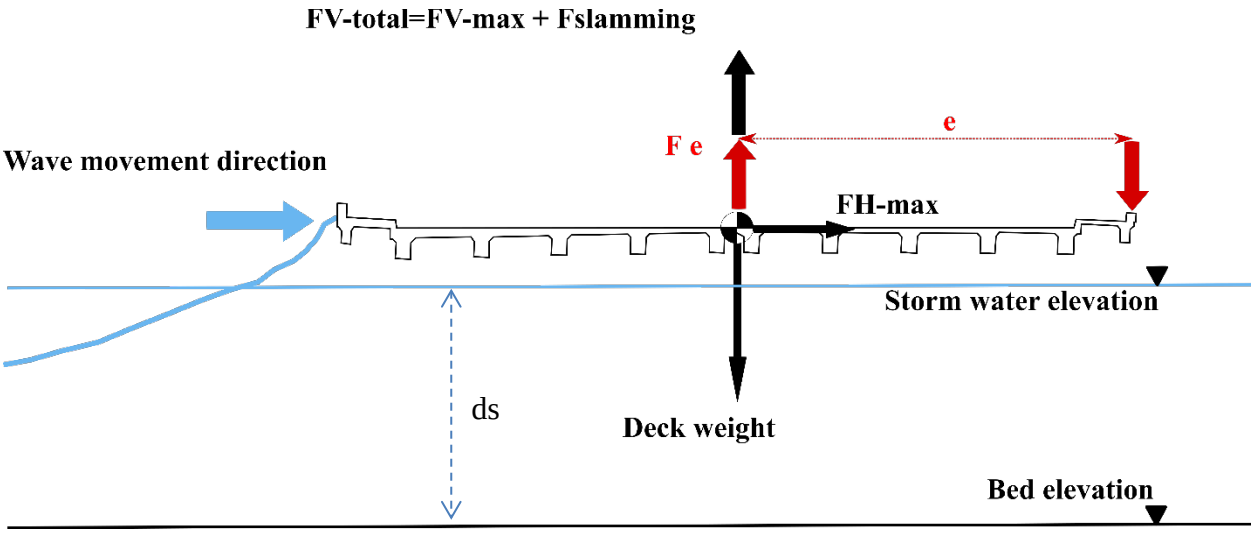

Figure 18 – Schematic Showing the Free-body Diagram of Forces Imposed on Bridge Superstructure.

It is recognized that culverts are not analyzed further because they must be analyzed based on the characteristics of open channel flow and that the AASHTO Guide provides no guidance for such analysis. The 353 bridges identified during the initial screening include 91 culverts. Therefore, 262 bridges are identified vulnerable from initial screening. For the purpose of hurricane vulnerability assessment, culverts may be considered vulnerable when submerged and thus are not further analyzed as a part of this study.

5.2 Results

It is concluded from the Level I analysis that the self-weight is not sufficient to resist the vertical wave force in 295 bridges for Category 5 hurricanes. Additional 33 bridges are identified by this Level-I analysis. Therefore, all of the 295 bridges (not including culverts) identified vulnerable in this section will be reconsidered for the Level-II analysis to account for the eccentric loads and

capacity of bearing connections. Table 6 summarizes the results, and Fig. 19 illustrates the results from the Level-I analysis (i.e., locations of failed bridges).

Table 6 – The Number of Bridges by Owners Considered Failed Using the Level I Method.

Method of Evaluation	Owner	Number of bridges considered failed				
		CAT 1	CAT 2	CAT 3	CAT 4	CAT 5
AASHTO Level 1 (High Tide)	State Highway Agency	21	105	155	180	211
	County Highway Agency	22	45	63	65	66
	City/Municipal Highway Agency	1	5	8	11	17
	State Park/Forest/ Reservation	0	1	1	1	1
	Total	**44**	**156**	**227**	**257**	**295**

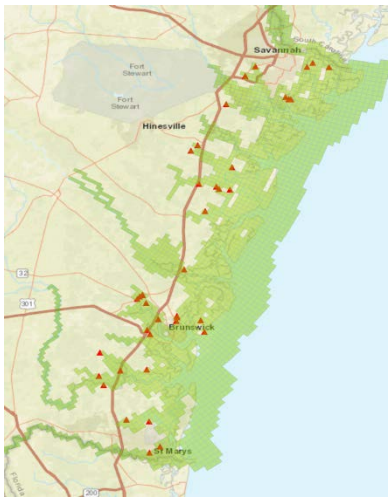

(a) Category 1

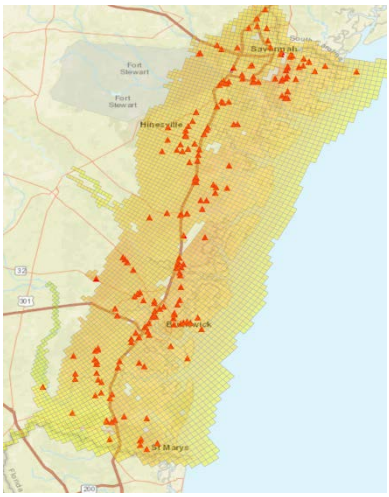

(d) Category 4

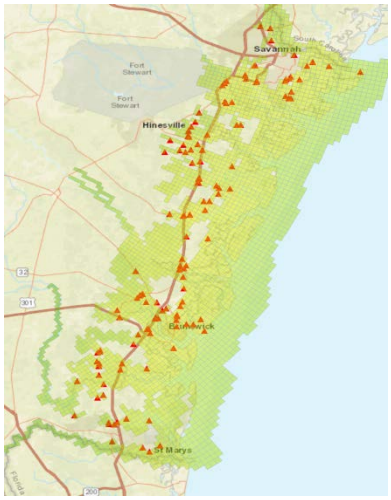

(b) Category 2

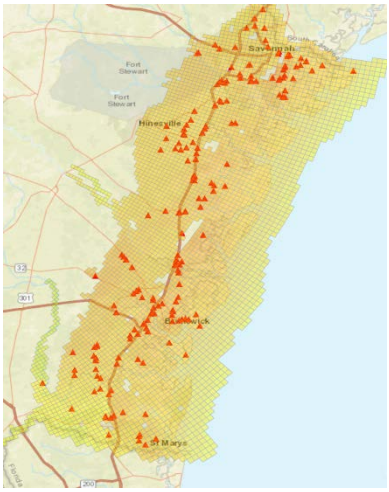

(e) Category 5

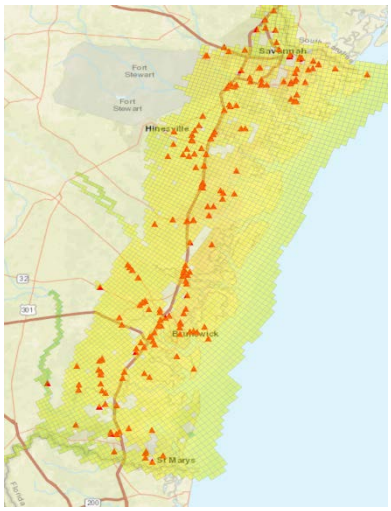

(c) Category 3

(note) Failed bridges are indicated by the red ‘triangle’ symbol

Figure 19 - Bridges Considered Failed by Level I Analysis.

5.3 Discussion of the Level I Results

In this approach, it should be recognized that bridges with anchor bolt connections are considered failed so long as the vertical force computed by the AASHTO code exceeds the weight of superstructure. In the following section (i.e., discussion of Level II analysis), bridges with such connections may or may not be determined most vulnerable. Approximately 80% of the failed bridges are simply supported concrete bridges (e.g., T-beam or prestressed), which warrants the Level II assessment. However, a majority of the bridges pertain dowel connections as shown in Table 7 and thus provide no additional vertical strength beyond the self-weight of superstructure. That is, the bridges will also fail by the Level-II analysis.

Table 7 – The Number of Bridges by Connection Types Considered Failed Using Level I.

Method of Evaluation	Super-Substructure Connection Type	Number of bridges considered failed				
		CAT 1	CAT 2	CAT 3	CAT 4	CAT 5
AASHTO Level 1 (High Tide)	Dowels	38	131	185	199	219
	Anchor Bolts	6	19	32	47	65
	Others (e.g., dowels & anchors)	0	6	10	11	11
	Total	**44**	**156**	**227**	**257**	**295**

Figure 20 shows an overlap of two map layers showing vulnerable bridges (see the red triangle symbols) resulting from the Level-I analysis, as well as all of the coastal bridges by bearing connection types. As seen in the figure, bridges are considered failed regardless of connection types (where the red 'triangle' symbols overlap with both green and blue 'diamond' symbols). 65 bridges which include anchor bolt connections are considered failed in this analysis; however, these 65 bridges will be re-evaluated in the Level II assessment. The connection types are further discussed in Section 6.3.2 (or Discussion of the Level II Results).

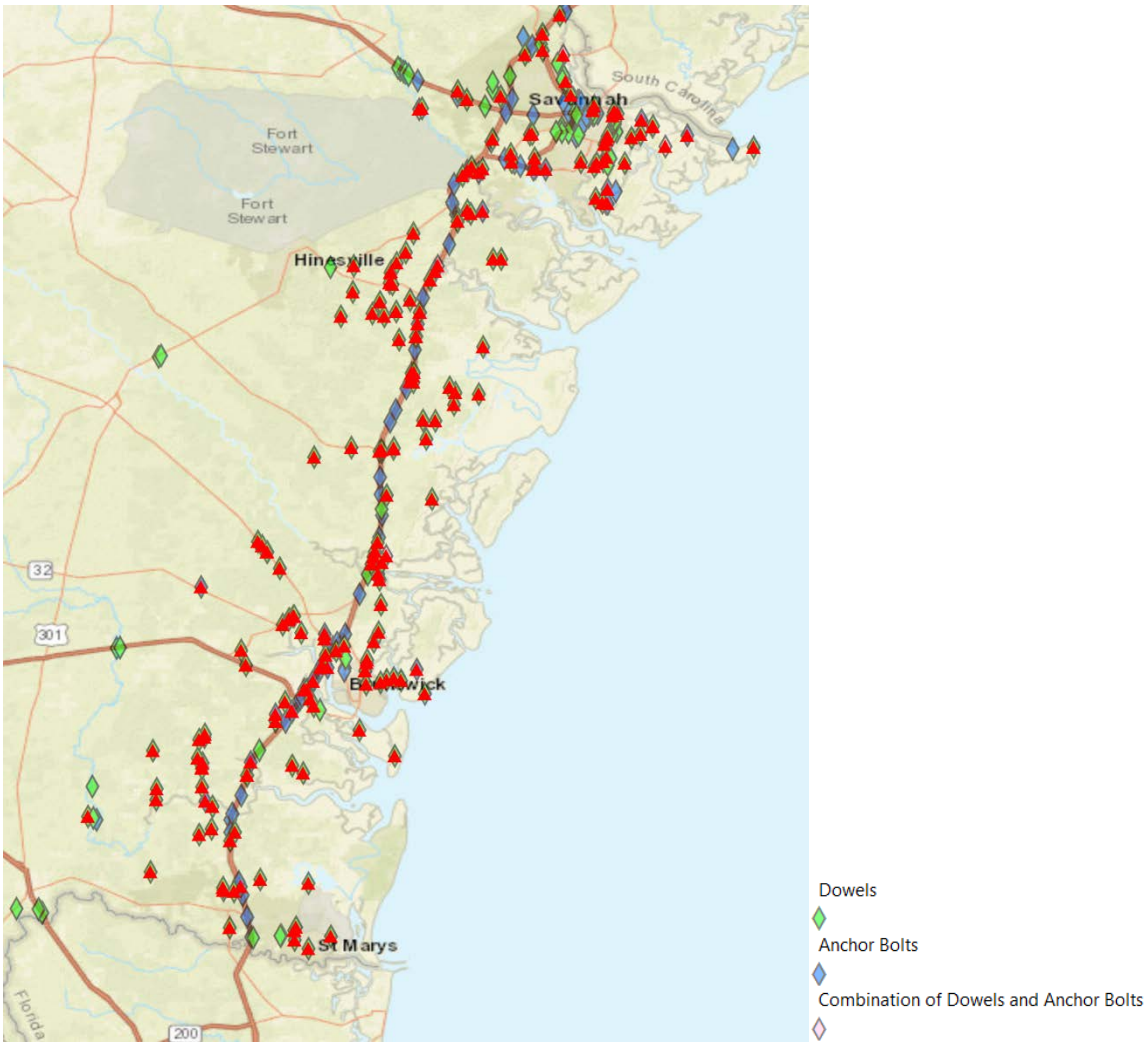

Figure 20 – Level-I Failed Bridges by Bearing Connection Types.

(Note: Failed bridges are indicated by the red ‘triangle’ symbol).

6. LEVEL II ASSESSMENT

6.1 Methodology

6.1.1 AASHTO Level II Assessment Method

The Level II analysis considers a more detailed force analysis (including associated moments and horizontal forces) for water level and wave conditions to identify potentially vulnerable coastal bridges in Georgia, and thus may result in less conservative and more accurate outcomes relative to the Level I assessment.

6.1.2 Methodology Used to Determine the Probability of Failure

The operational status of bridges is generally evaluated in terms of reliability of representative bridges. Because reliability is a probabilistic measure, analysis of bridge structures will incorporate a statistical method to account for uncertainties. That is, the statistical analysis will incorporate fragility curves that relate reliability of a component with measurable environmental parameters (i.e., wind speed, water depth, flow velocity, wave height, etc.). The probability of failure for each bridge will be determined, and a sortable database which presents a list of bridges with the highest risk of damage (or failure) for the five hurricane categories will be created.

In this method, the two components are critically important to determine bridge vulnerability: (1) the cause of a failure mode and (2) the probability of failure occurrence. The potential causes or a failure mode are identified from a nonlinear structural analysis (e.g., weight of superstructure and connection types including dowel/bolt size, and/or elevation of superstructure). Each bridge is given a probability of failure (or vulnerability score) by completing the following 12 steps (Saeidpour 2017):

Step 1: Determine the storm water elevation, 'ds' for each hurricane category using the SLOSH high tide storm water elevations.

Step 2: Determine the peak spectral period, T_P, and significant wave height, H_s, using the AASHTO Guide.

Step 3: Generate the 'n1' number of samples from a uniform storm water elevation distribution using the Latin Hypercube Sampling (LHS) method.

Step 4: Obtain a wave spectrum using the three parameters determined in Steps 1 through 3. It is recognized that the TMA spectrum (Battjes et al. 1987) is adopted. The wave spectrum, illustrated for a selected bridge in Fig. 21, is used to determine the wave height and period distributions presented in Steps 5 and 6. Figures 22 and 23 illustrate the distributions.

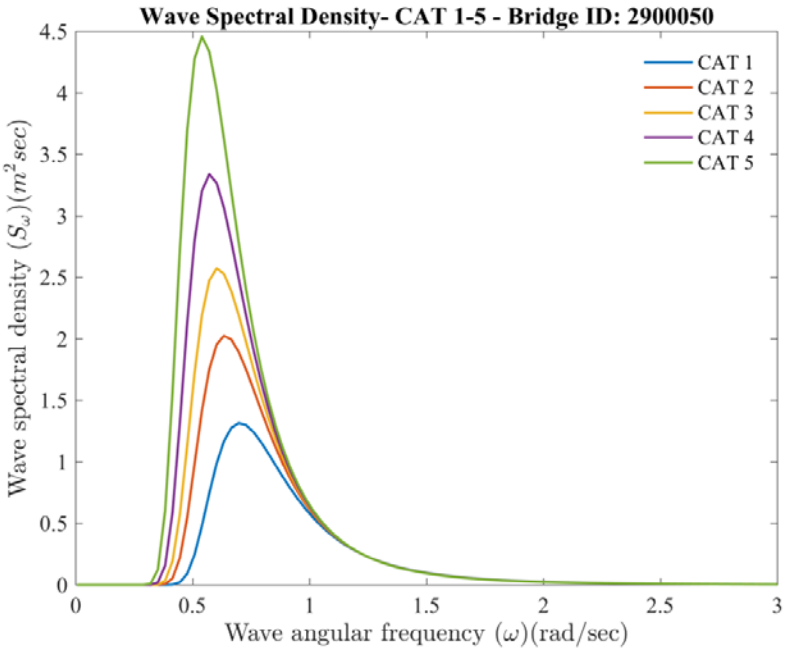

Figure 21 – Sample Wave Spectra.

Step 5: Generate the ‘n1’ number of wave amplitude samples from the wave height, ‘H’, distribution (Klopman 1996) using the Latin Hypercube Sampling (LHS) method.

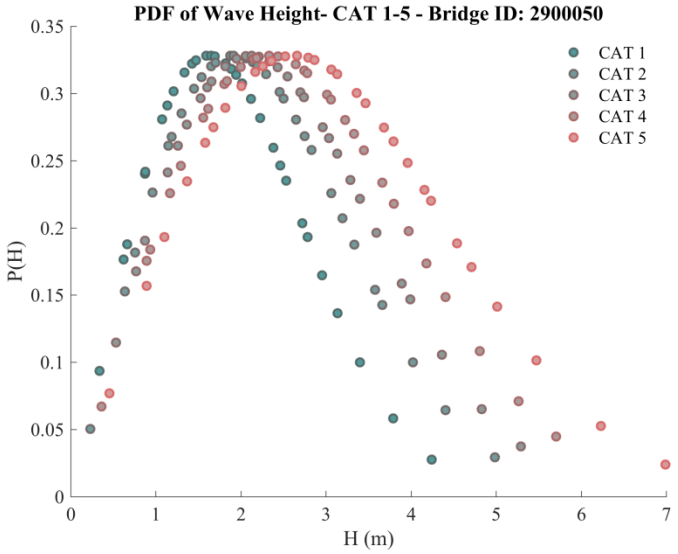

Figure 22 – Sample probability distribution of wave height.

Step 6: Generate the ‘n2’ number of wave period samples from the wave period, ‘T’, distribution (Le Mehaute 1986) using the Latin Hypercube Sampling (LHS) method.

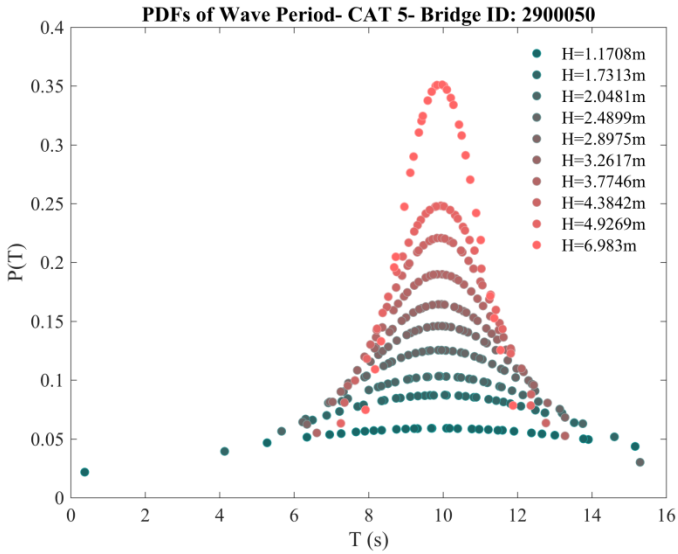

Figure 23 – Sample probability distribution of wave period.

Step 7: A uniform distribution of the SLOSH surge height (with +/- 20% uncertainty) is considered, and the LHS method is used to generate 'n1' x 'n2' random samples. The uncertainty inherent in the calculation of wave height and period, which directly affects the magnitude of hurricane wave forces is incorporated in the fragility analysis.

Step 8: With a set of the storm water elevation, wave height, and wave period determined for varying wind speed (U_{10min}), it is possible to determine wave (quasi-static vertical, slamming, and horizontal) forces, in accordance with the AASHTO Guide.

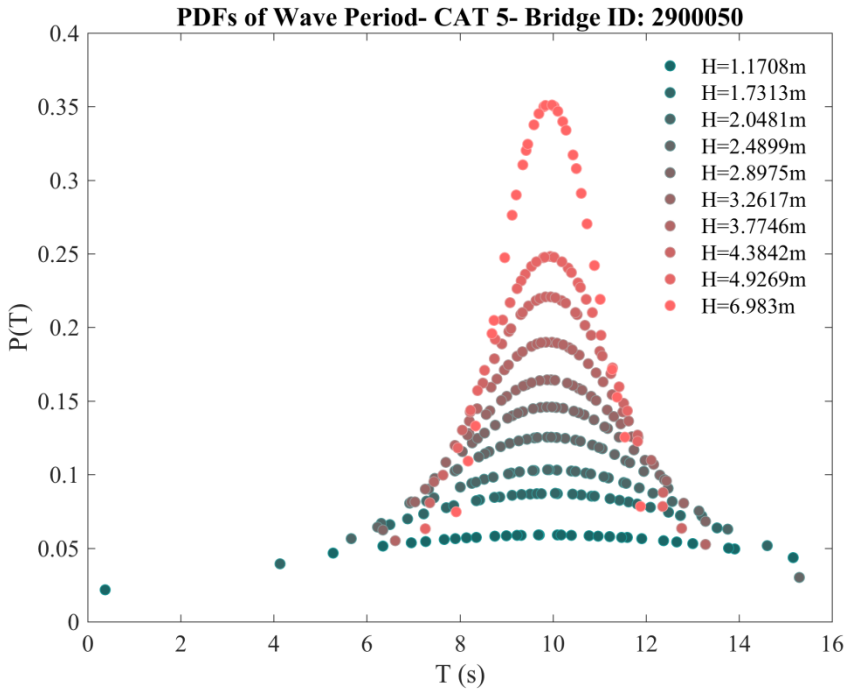

Figure 24 – Sample fragility curves.

(note): The fragility curves describe the probability of distribution as a function of T and H for the Category 5 threshold wind speed.

Step 9: An OpenSees bridge model, similar to shown in Fig. 25, is constructed for each bridge, and the wave forces determined from Step 8 are applied. A time-history nonlinear analysis is conducted. A sample time-history of the wave forces applied to each bridge model is illustrated in Fig. 26.

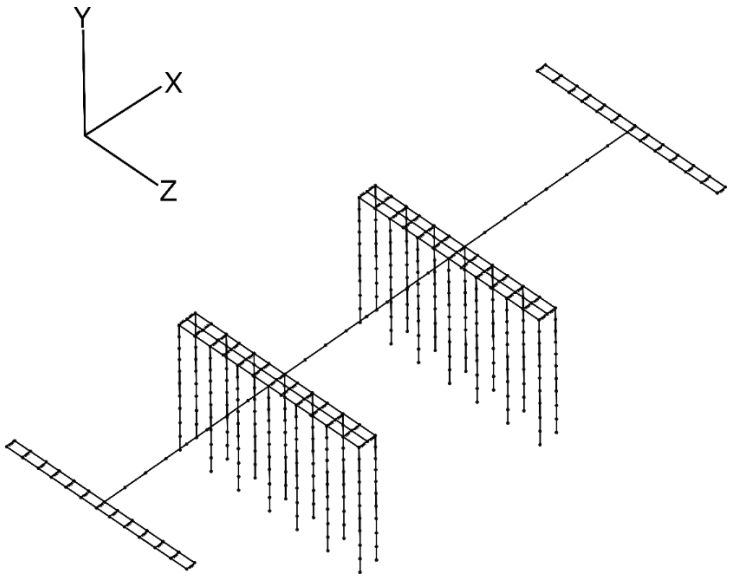

Figure 25 – Sample bridge analysis model developed in the OpenSEES software.

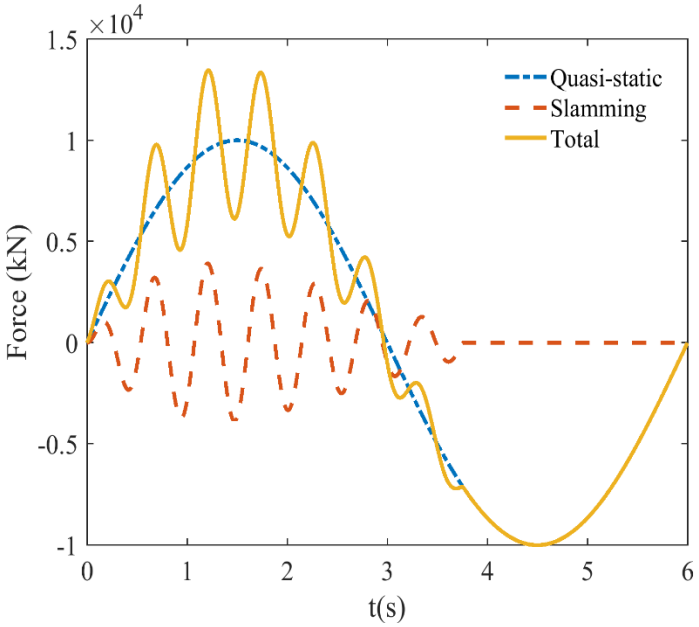

Figure 26 – Time (in second) history of wave forces on the bridge deck section.

Step 10: The probability of failure for the 'i'th bridge span is determined by the following equation:

$$P_{f_{span}}^{i} = P_{f_{span}}^{i}(D - C > 0|IM) \quad (28)$$

, where D is the demand; C is the capacity; and IM: Hazard Intensity Measure

In this study, the probability of failure is conditioned on U_{10min} and determined at incremental levels of wind speed (or U_{10min}) by Eq. (29):

$$P_{f_{span}}^{i} = P_{f_{span}}^{i}(D - C > 0|U_{1-min}) = \Phi\left(\frac{\ln(U_{1-\min})-\hat{\mu}}{\hat{\beta}}\right) \quad (29)$$

, where D is the demand; C is the capacity; U_{10min} is the 10-minute wind speed; Φ is the standard normal cumulative distribution function; and $\hat{\mu}$ and $\hat{\beta}$ are the mean and standard deviation.

This study uses the maximum likelihood method to find $\hat{\mu}$ and $\hat{\beta}$ from the observed probability of failure (Baker 2015).

Step 11: The probability of bridge failure (as a series system) is determined by the following equation, where 'N' is the number of spans in a bridge:

$$P_{f_{Bridge}} = 1 - \prod_{i=1}^{N}(1 - P_{f_{span}}^{i}) \quad (30)$$

Step 12: A fragility curve which describes the probability of failure for a wide range of wind speeds is constructed. At each wind speed, a total of 900 bridge simulations are conducted to determine the probability of failure where n1=30 and n2=30 are selected.

$$\frac{\sum_1^{n_{total}} \mathbf{1}(D-C)}{n_{total}} \tag{31}$$

, where 'n' is the number of simulations for each wind speed (i.e., n = 900); and $\mathbf{1}()$ is the binary indicator function defined as:

$$\mathbf{1}(x) := \begin{cases} 0 & x \geq 0, \\ 1 & x < 0. \end{cases} \tag{32}$$

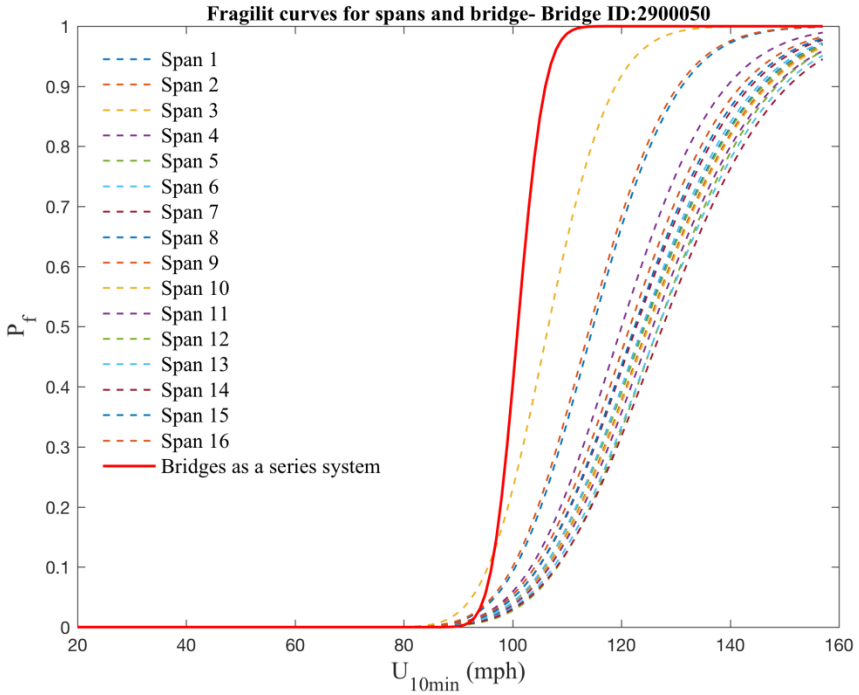

Figure 27 – Time-dependent wave forces.

Figure 27 illustrates a fragility curve for a 16-span bridge, where P_f is the probability of failure and U_{10min} is the 10-minute wind speed.

6.2 Results Expressed in Terms of the Probability of Failure

Table 8 provides a summary of the number of failed bridges for varying thresholds used to define a bridge failure. For Category 5 hurricanes, the number of failed bridges does not change much between 80 and 95% thresholds. Based on this evaluation, it is reasonable to classify that bridges with the probability of greater than 95% are considered 'failed'. This 95% threshold also represents the most commonly used significance level of 0.05.

Table 8 – The Number of Bridges by Probability of Failure Thresholds.

Method of Evaluation	Probability of Failure Threshold	Number of bridges considered failed				
		CAT 1	CAT 2	CAT 3	CAT 4	CAT 5
AASHTO Level 2 (High Tide)	> 80 %	43	151	210	235	265
	> 90%	41	150	206	233	258
	> 95%	35	144	204	231	254

6.3 Discussion of the Results

In addition to the deck overtopping (or unseating) vulnerability, a rating of the bridge importance (to GDOT) and other factors may be employed within a decision matrix to determine the probability of failure (or vulnerability).

In case of the Category 5 analysis results, it is discovered that 26 bridges with anchor bolts (refer to Table 10) are removed from the 'failed' or most vulnerable bridge list because of additional vertical resistance provided by the tensile capacity of anchor bolts. The nonlinear response of bridges considered in the analysis (see Section 6.1.2) is one of the reasons for the reduction in the total number of bridges determined most vulnerable.

(a) Category 1

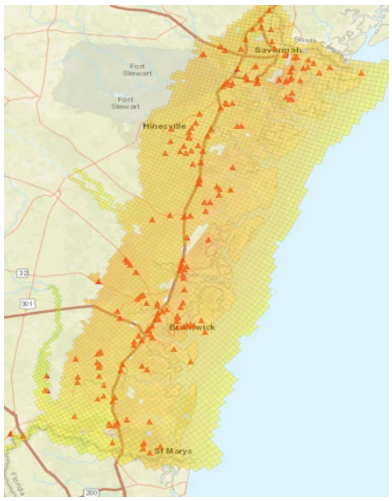

(d) Category 4

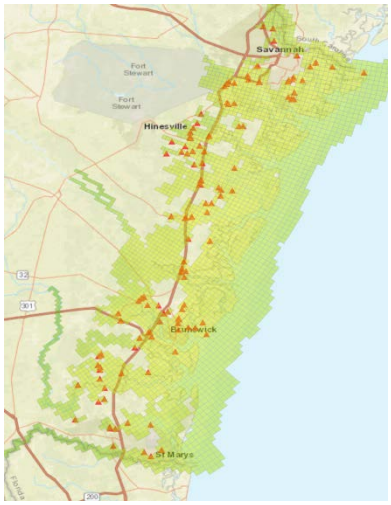

(b) Category 2

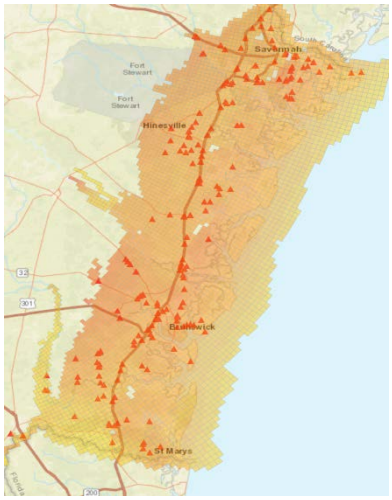

(e) Category 5

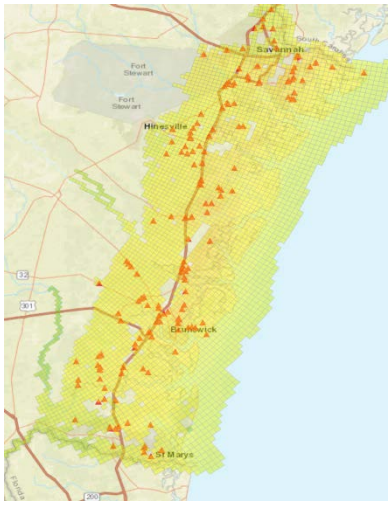

(c) Category 3

Figure 28 - Vulnerable Bridges (>95% probability of failure) by Level II Assessment.

6.3.1 Bridge Owners

Approximate 70% of potentially vulnerable bridges are owned by the state highway agency (or GDOT), as shown in Table 9 and illustrated in Fig. 29.

Table 9 – The Number of Bridges Vulnerable by Owners.

Method of Evaluation	Owner	Number of bridges considered failed				
		CAT 1	CAT 2	CAT 3	CAT 4	CAT 5
AASHTO Level 2 (High Tide)	State Highway Agency	16	94	137	159	179
	County Highway Agency	18	45	58	63	65
	City/Municipal Highway Agency	1	4	8	8	9
	State Park/Forest/ Reservation	0	1	1	1	1
	Total	**35**	**144**	**204**	**231**	**254**

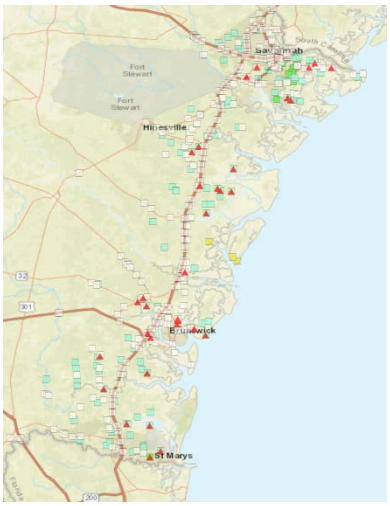

(a) Category 1

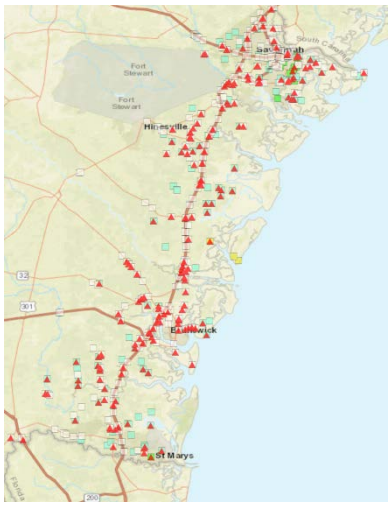

(d) Category 4

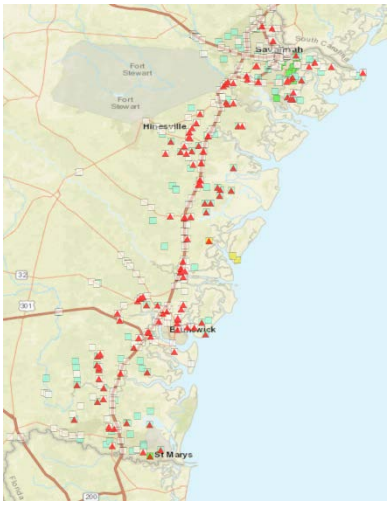

(b) Category 2

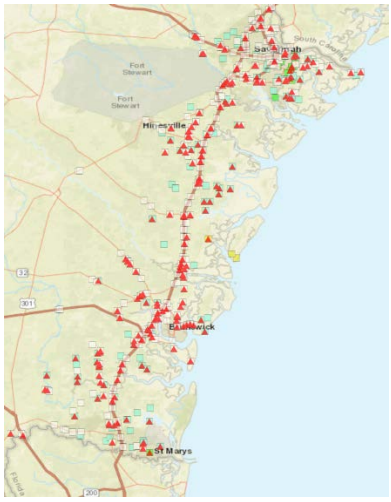

(e) Category 5

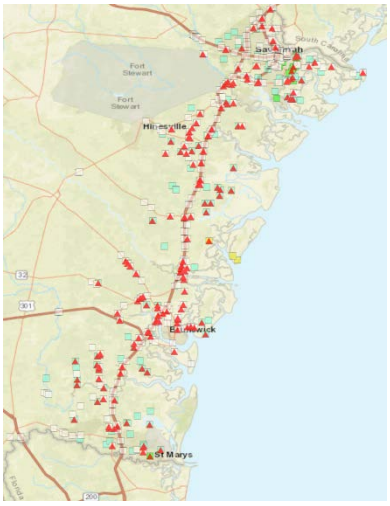

(c) Category 3

Legend:

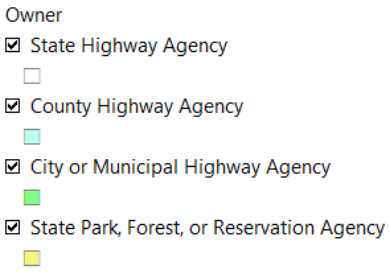

Figure 29 - Potentially Vulnerable Bridges and Coastal Bridges by Owners.

6.3.2 Super-to-Substructure Connection Types

Figure 30 shows the location of vulnerable bridges by bearing connection types. At large, bridges with dowel bar connections fail whereas bridges with anchor bolts may or may not fail. It should be recognized that the consideration of tensile capacity of anchor bolts has significantly reduced the number of failed bridges as shown in Table 10. For instance, the number of failed bridges (with anchor bolt connections) has reduced by 10 bridges (from 32 to 22 bridges) for Category 3 hurricanes due to additional tensile capacity. The bolt/anchor shear failure is not the primary mode of failure as the anchor tensile failure occurs before shear failure develops for the size of anchor bolts considered in this study.

Table 10 – Potentially Vulnerable Bridges by Connection Types.

Method of Evaluation	Super-Substructure Connection Type	Number of bridges considered failed				
		CAT 1	CAT 2	CAT 3	CAT 4	CAT 5
AASHTO Level 1 (High Tide)	Dowels	38	131	185	199	219
	Anchor Bolts	6	19	32	47	65
	Others (e.g., dowels & anchors)	0	6	10	11	11
	Total	**44**	**156**	**227**	**257**	**295**
AASHTO Level 2 (High Tide)	Dowels	33	128	173	194	204
	Anchor Bolts	2	11	22	26	39
	Others (e.g., dowels & anchors)	0	5	9	11	11
	Total	**35**	**144**	**204**	**231**	**254**

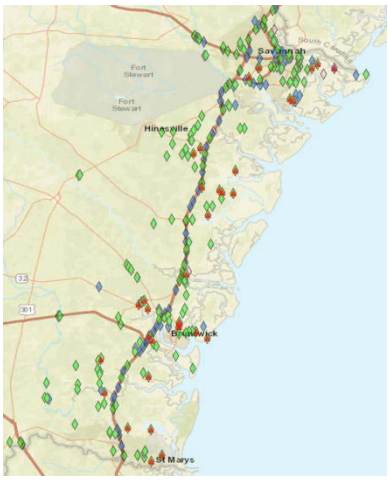

(a) Category 1

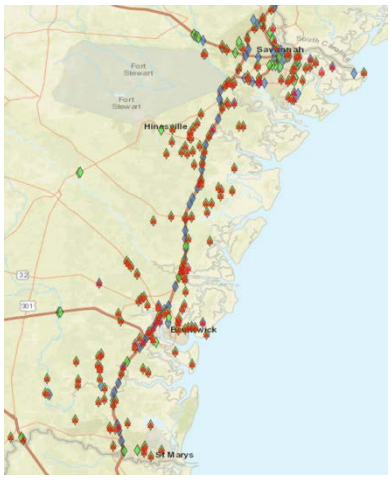

(d) Category 4

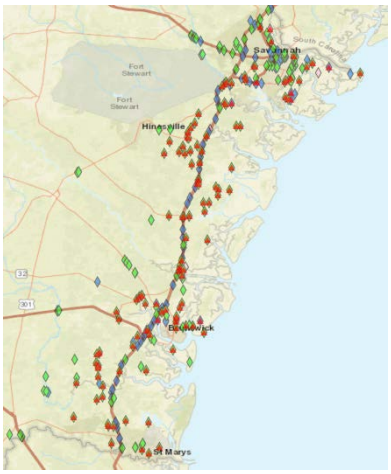

(b) Category 2

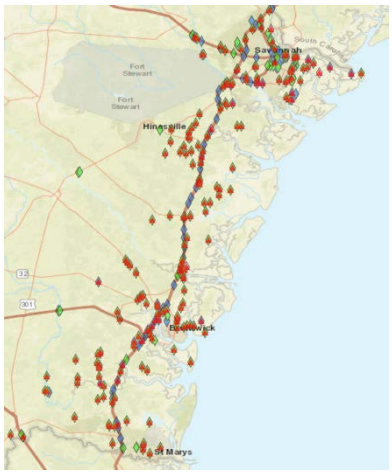

(e) Category 5

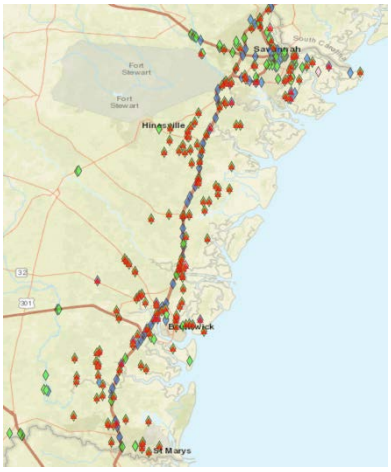

(c) Category 3

Legend:

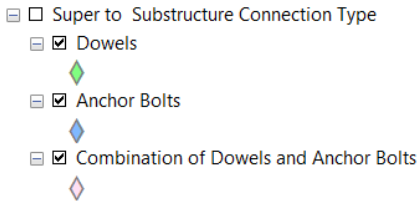

Figure 30 - Potentially Vulnerable Bridges and Coastal Bridges by Connection Types.

6.3.3 Superstructure Types

Table 15 shows that vulnerable bridges are made of concrete, regardless of pre-stressed or reinforced. Figure 31 includes the two map layers displaying the locations of failed bridges and bridges by connection types using the ArcMap software.

Table 11 – Potentially Vulnerable Bridges by Superstructure Types.

Method of Evaluation	Super-structure Type	Number of bridges considered failed				
		CAT 1	CAT 2	CAT 3	CAT 4	CAT 5
AASHTO Level 2 (High Tide)	Prestressed Conc Channel Beam	0	0	3	3	3
	Prestressed Slab	0	2	2	2	2
	Prestressed Concrete Girder/ Floor beam	11	32	51	59	65
	Concrete Slab	12	28	36	41	41
	Concrete Tee Beam	9	65	90	98	104
	Steel Continuous Girder	1	6	10	11	15
	Steel Girder/Floor beam	0	0	0	4	9
	Others	2	7	8	9	11
	Total	**35**	**144**	**204**	**231**	**254**

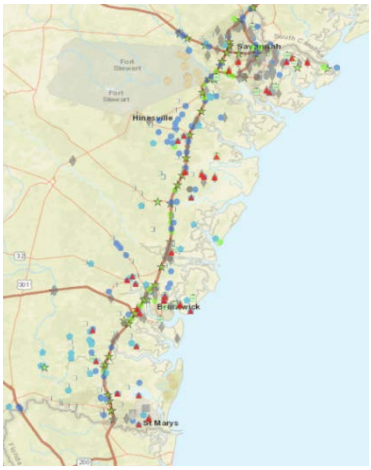

(a) Category 1

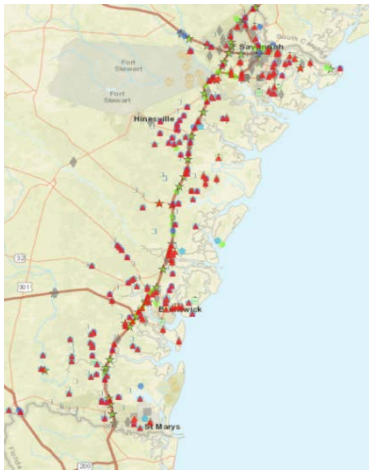

(d) Category 4

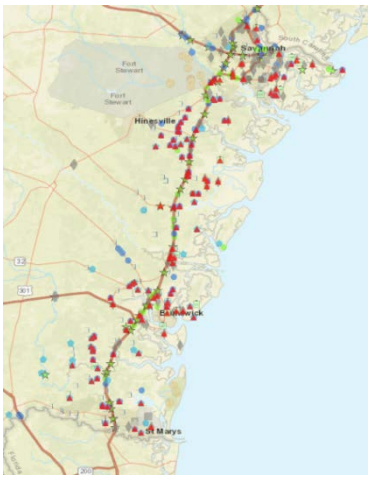

(b) Category 2

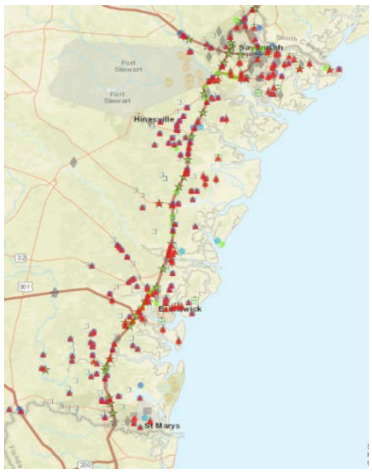

(e) Category 5

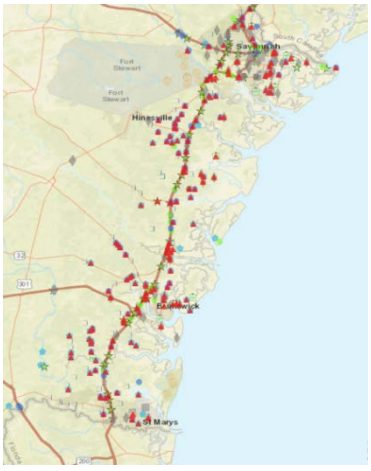

(c) Category 3

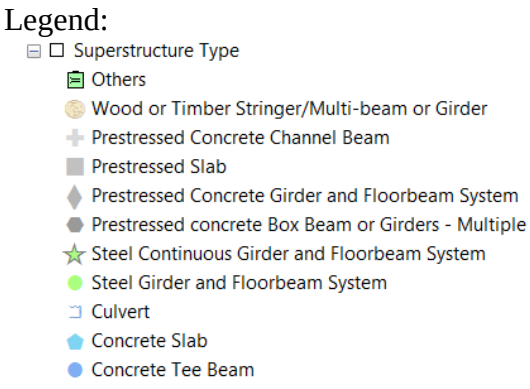

Figure 31 - Potentially Vulnerable Bridges and Coastal Bridges by Superstructure Types.

6.3.4 Year Constructed

Table 12 presents the number of vulnerable bridges by year constructed. Regardless of the year constructed, bridges remain vulnerable to hurricane events, noting that the coastal bridges included in this analysis are obtained in August 2015, which explains the absence of bridges constructed between 2011 and 2014. Figure 32 includes two map layers showing the locations of failed bridges identified by the Level-II analysis as well as all coastal bridges by year constructed.

Table 12 - Potentially Vulnerable Bridges by Year Constructed.

Method of Evaluation	Year Constructed	Number of bridges considered failed				
		CAT 1	CAT 2	CAT 3	CAT 4	CAT 5
AASHTO Level 2 (High Tide)	1922-1940	0	1	1	1	1
	1941-1950	1	10	11	11	11
	1951-1960	8	35	41	46	48
	1961-1970	5	28	34	36	47
	1971-1980	3	30	49	59	66
	1981-1990	13	19	24	26	27
	1991-2000	3	9	24	32	34
	2001-2010	2	12	20	20	20
	2011-2014	0	0	0	0	0
	Total	**35**	**144**	**204**	**231**	**254**

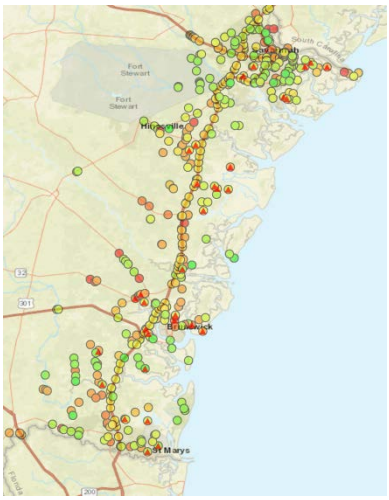

(a) Category 1

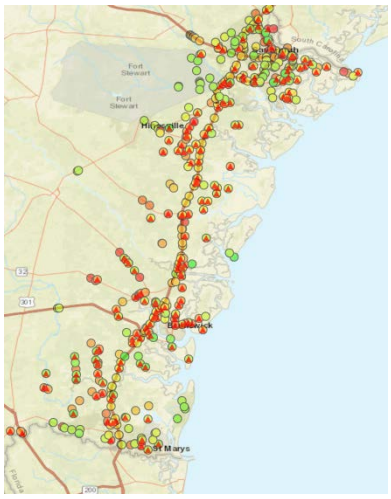

(d) Category 4

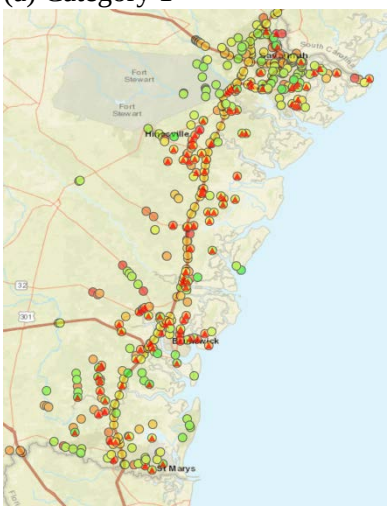

(b) Category 2

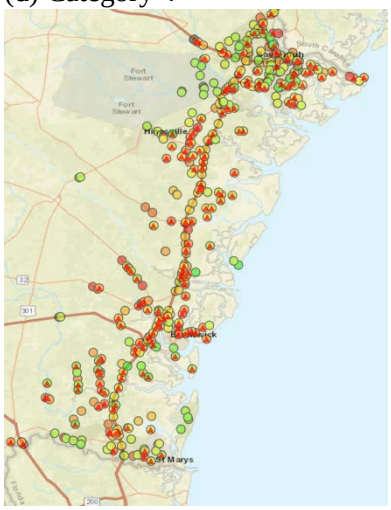

(e) Category 5

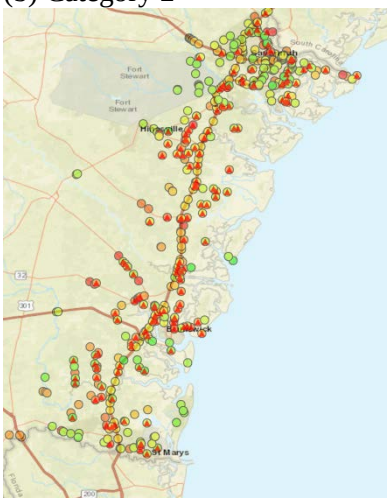

(c) Category 3

Legend:

Figure 32 - Potentially Vulnerable Bridges and Coastal Bridges by Year Constructed.

6.3.5 Hurricane Evacuation Route

The hurricane evacuation route published by GDOT is illustrated in Fig. 33, in conjunction with the analysis results (bridges with the probability of failure greater than 95%). Table 13 lists the bridge IDs and associated probabilities of failure.

Table 13 – Potentially Vulnerable Bridges on the Hurricane Evacuation Route.

Method of Evaluation	Bridge ID	Probability of Failure (%), rounded to the nearest ones place				
		CAT 1	CAT 2	CAT 3	CAT 4	CAT 5
AASHTO Level 2 (High Tide)	2900240	0	0	95	100	100
	2900310	0	0	0	0	96
	2900330	0	0	0	0	100
	2900340	0	0	0	0	100
	2900510	0	100	100	100	100
	2900520	0	100	100	100	100
	4900020	0	0	0	100	100
	5100320	0	100	100	100	100
	5100330	0	99	100	100	100
	5100630	100	100	100	100	100
	5100650	97	100	100	100	100
	5100710	0	0	47	100	100
	5100730	0	99	100	100	100
	5100760	0	0	1	78	100
	5100820	0	0	96	100	100
	5100830	0	0	96	100	100
	5101630	0	10	85	100	100
	10300230	0	0	0	7	100
	10300240	0	0	0	10	100
	12700220	0	0	100	100	100
	12700230	0	100	100	100	100
	12700270	100	100	100	100	100
	12700280	92	100	100	100	100
	12700290	93	100	100	100	100
	12700310	88	100	100	100	100
	12700320	95	100	100	100	100
	12700340	0	100	100	100	100
	12700720	0	100	100	100	100
	12700780	0	2	93	100	100
	12750100	0	21	100	100	100
	12750110	0	30	100	100	100
	12750120	0	20	100	100	100
	12750130	0	7	100	100	100
	12750140	0	21	100	100	100
	12750150	0	7	100	100	100
	12750160	0	92	100	100	100
	12750170	0	91	100	100	100
	12750180	0	3	93	100	100
	17900200	0	100	100	100	100
	Total count-bridges w $P_f > 95\%$	**4**	**16**	**28**	**33**	**39**

(a) Category 1

(b) Category 2

(c) Category 3

(d) Category 4

(e) Category 5

Figure 33 - Potentially Vulnerable Bridges on the Hurricane Evacuation Route.

6.4 Hazard Risk Assessment

Hurricane risk analysis of bridges enables the stakeholders of GDOT to assign their resources to the most critical bridges in the inventory through a risk-informed decision making process. For the risk assessment procedure, it is necessary to define a probabilistic model for hurricane hazard, which describes the frequency of the hazard occurrence as a function of an intensity measure (i.e., maximum sustained wind speed). The return period of hurricane wind speed proposed by Vickery et al. (2009) is used for a risk assessment. Vickery et al. proposed a hurricane simulation model by using historical data of past hurricanes. In this model, numerous hypothetical hurricane tracks were generated for hurricane prone coastal regions of the United States and simulated using the statistical distributions derived from the inventory of past hurricanes and estimates of wind speed as a function of return period. The ASCE-7 wind speeds and HAZUS hurricane model are based on the model developed by Vickery et al.

Under this model, the maximum threshold wind speed for each hurricane category in the Saffir-Simpson scale is correlated to its associated SLOSH MOM surge height. Wind speeds provided by Vickery et al. are the 3-sec peak gust wind speeds, and thus are converted to the 1-min averaged sustained wind speed, which also has been used as the hazard Intensity Measure (IM) for the proposed fragility analysis. Finally, the risk is quantified in terms of the mean annual rate of bridge failure (AMR_{Bridge}):

$$AMR_{Bridge} = \int \left(\frac{dP_{f_{Bridge}}}{dU_{1min}}\right) AMR_{U1min} dU_{1min} \quad (33)$$

in which $P_{f_{Bridge}}$ is the fragility function, and AMR_{U1min} is the mean annual rate of exceedance for the sustained wind speed.

6.4.1 Hazard Curve

Figure 34 shows the maximum hurricane 3-sec peak gust wind speed and return period along the coast of Georgia and South Carolina (Vickery et al. 2009). To obtain the hazard curve shown in Fig. 35, which is needed to take the integral in Eq. (33), the 3-sec peak gust wind speed was converted to the 1-min averaged sustained wind speed using equations provided in the AASHTO Guide. In addition, the return period is converted to the mean annual rate of occurrence, AMR_{U1min}. Fragility curves of bridges obtained in the previous sub-section and hazard intensity curve shown in Fig. 35 are used in Eq. (33) to obtain the mean annual rate of failure ($\mathrm{AMR}_{\mathrm{Bridge}}$) for each bridge.

6.4.2 Mean Annual Rate of Failure or Risk

Figure 36(a) illustrates the mean annual rate of failure, $\mathrm{AMR}_{\mathrm{Bridge}}$, for Georgia's coastal bridges on a map. It is concluded that seventeen bridges have the mean annual rate of occurrence, $\mathrm{AMR}_{\mathrm{Bridge}}$, greater than 0.1, and they are all located within 5km from the shoreline as presented in Fig. 36(b).

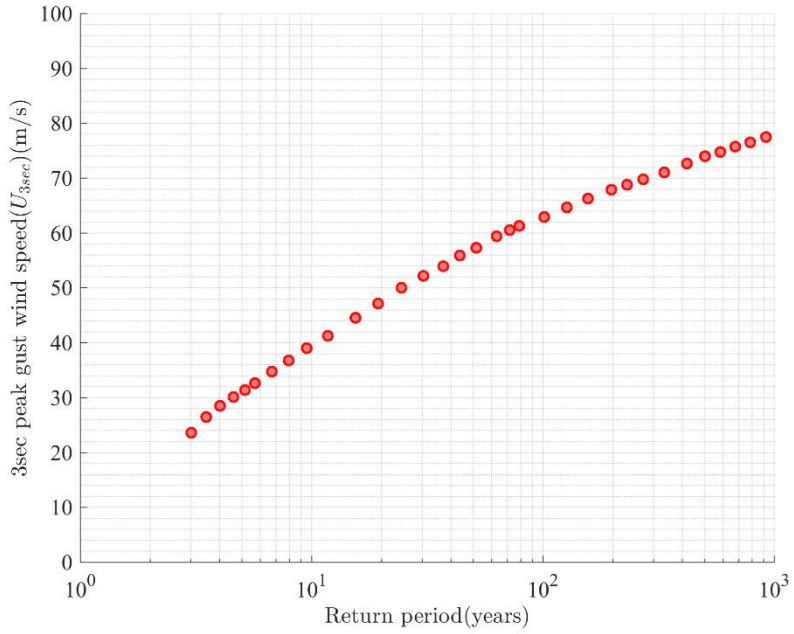

Figure 34 - Maximum hurricane induced 3-second peak wind speeds over land along GA/SC coastline versus return period (Vickery et al. 2009).

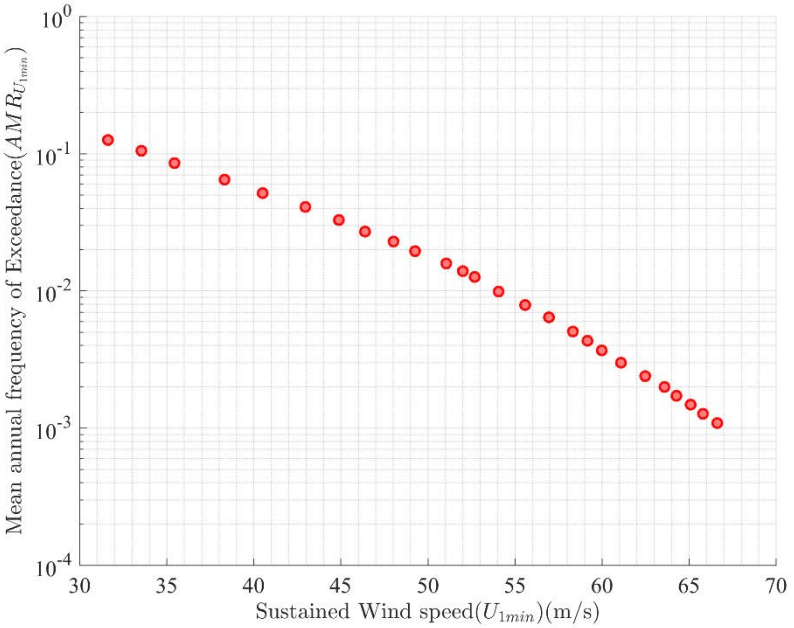

Figure 35 - Mean Annual Frequency of Exceedance and Sustained Wind Speed.

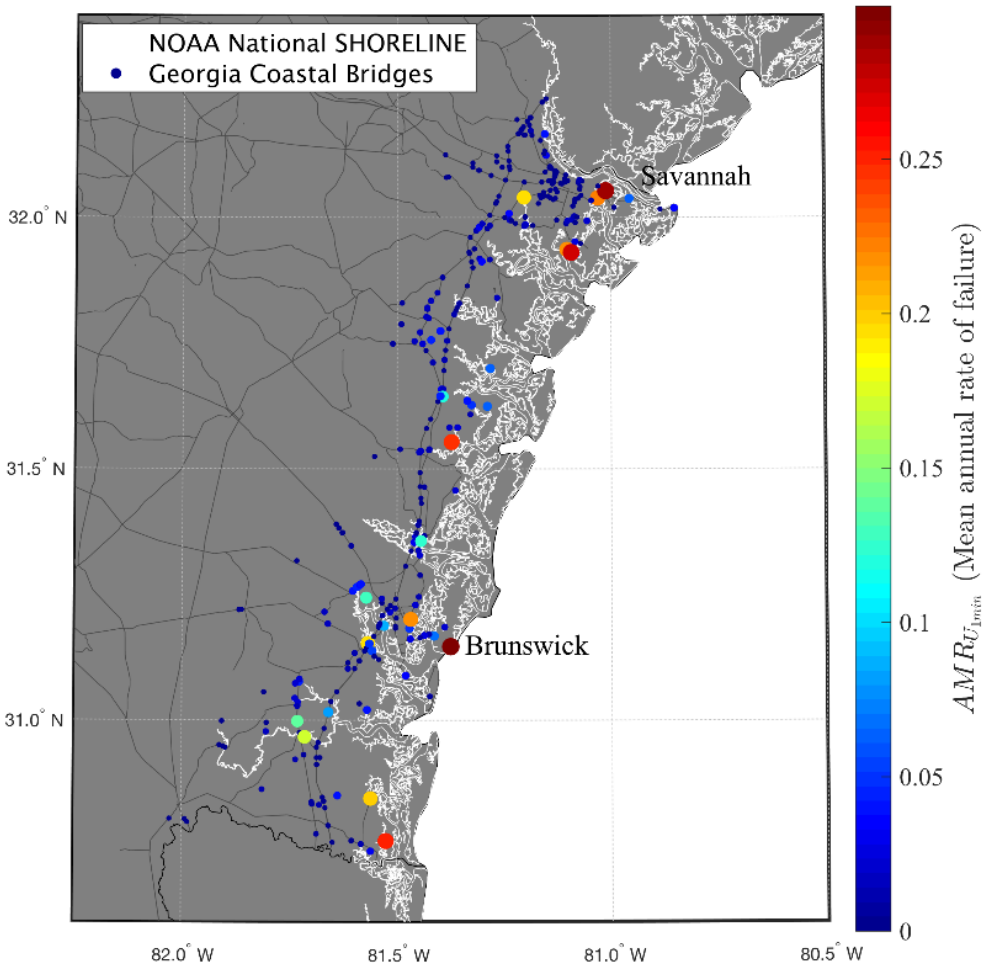

(a) Mean Annual Rate of Failures and Bridge Locations.

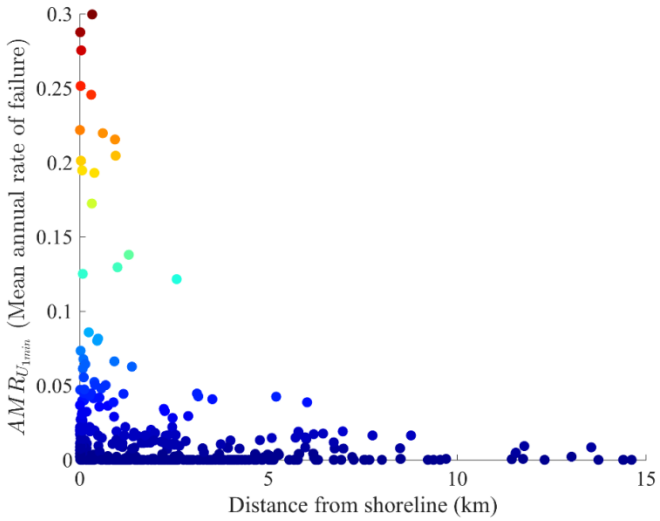

(b) Mean Annual Rate of Failure and Distance From the Shoreline.

Figure 36 - Mean Annual Rate of Failure.

Table 14 – Seventeen bridges with the mean annual rate of failure greater than 0.1.

Method of Evaluation	Bridge ID	Mean Annual Rate of Bridge Failure	NBI Designation		
			Owner	Structure Kind	Structure Type
Risk Assessment					
	12750040	0.130	2(county)	1(concrete-simple)	1(Slab)
	3950470	0.172	2(county)	1(concrete-simple)	1(Slab)
	3950290	0.201	2(county)	1(concrete-simple)	1(Slab)
	5101450	0.220	2(county)	5(pre-stressed conc. simple)	2(Multi-Beam)
	19150040	0.246	2(county)	1(concrete-simple)	1(Slab)
	3950510	0.251	2(county)	5(pre-stressed conc. simple)	2(Multi-Beam)
	5150080	0.276	2(county)	1(concrete-simple)	1(Slab)
	5150130	0.288	2(county)	5(pre-stressed conc. simple)	2(Multi-Beam)
	12750030	0.300	2(county)	1(concrete-simple)	1(Slab)
	Total count	**17 bridges**			

6.4.3 Analysis of Bridges at Comparatively Higher Risk

The bridges with the mean annual rate of failure of 0.1 indicate that there is more than 10% chance that a given bridge will fail during a year of use. The seventeen bridges with the mean annual rate of bridge failure greater than 0.1 are simply supported concrete or pre-stressed concrete bridges with an exception of two bridges, one continuous steel bridge and the other continuous reinforced concrete slab bridge. Five bridges are simply supported prestressed concrete bridges and nine bridges are simply-supported reinforced concrete bridges. It should be recognized that wave forces for continuous spans are conservatively estimated based on the assumption under which bridge spans could independently fail. Therefore, it is expected the mean annual rate of bridge failure should be much lower than 0.195 and 0.205 estimated for the continuous steel and concrete bridge, respectively, when a detailed analysis is conducted.

Eight bridges (of 18 bridges) are owned by the state, and the remaining nine bridges are county-owned. The five simply supported prestressed concrete bridges consist of multiple girders, and the nine simply-supported reinforced concrete bridges consist of either T-beam or slab sections.

7. IMPLEMENTATION AND DELIVERABLES

The study team has organized the project deliverables into three categories in the following sub-sections. Tables 15 through 17 illustrate the database provided in excel format.

7.1 BridgeWatch Input Needed

The GDOT has a BridgeWatch software license and thus requested that the research team deliver the following information for its hurricane module:

1. When does GDOT alert potential vulnerability? (i.e., threshold value)

   As discussed in Section 2.1, the AASHTO Guide provides the answer to this question: "vertical clearances of highway bridges should be sufficient to provide at least 1 foot of clearance over the 100-yr design crest elevation, which includes the design storm water elevation"

2. When do bridge superstructures get wet?

   The fourth column in Table 15 summarizes the lowest elevation in each bridge. Table 16 illustrates a summary of raw elevation survey data in which multiple locations including approach locations are presented for each bridge. Section 4 provides a summary of submerged bridges utilizing the SLOSH MOM data.

3. When do bridge components fail (e.g., the threshold probability of failure measure)?

   Table 15 illustrates the probability of failure determined for each bridge corresponding to each hurricane category. The threshold probability is 0.95. Section 6 provides a summary of bridges considered failed using the threshold (of 0.95).

Furthermore, the mean and standard deviation, $\hat{\mu}$ and $\hat{\beta}$ in Eq. (29) necessary to characterize a fragility curve are provided for each bridge.

Table 15 – BridgeWatch Input Used for This Study.

Bridge ID (NBI designation)	Survey Location (decimal format)		Survey Data (Lowest point)	Probability of Failure, P_f(%)				
*STRUCTURE_ NUMBER	Latitude	Longitude	Bridge Deck Top Surface Elev. (ft)	Category 1	Category 2	Category 3	Category 4	Category 5
2900350	31.90033865	-81.32350340	22.373	0.00	0.06	0.95	1.00	1.00
2900050	31.97746272	-81.29031241	16.796	0.00	0.09	0.99	1.00	1.00
2900320	32.13977668	-81.40964839	38.391	0.00	0.00	0.00	0.00	0.94

* (note): Three selected bridges are shown for illustration purpose only.

Table 16 – Elevation Survey (Raw Data).

Survey Location (decimal format)		Survey Results
Latitude	Longitude	Deck Top Surface Elev (ft)
*31.46369552	-81.43633599	13.255
31.91233710	-81.32581094	41.324
31.20059115	-81.46800362	8.413
31.20055131	-81.46784516	8.893
31.19585355	-81.46870441	8.407

* (note): Five selected rows are shown for illustration purpose only.

7.2 Master Database

The study team has created a master database in excel format in order to organize the bridge parameters including the connection details, SLOSH data, other resources, and analysis results such that GDOT staff and engineers are able to filter the data in a manner that corresponds to the agency's needs and goals.

Table 17 – Mater Database Including Important Parameters Used for This Study.

(Source) NBI	NBI	NBI	NBI	NBI	NBI	NBI	Bridge Plans	Bridge Plans	Bridge Plans	Bridge Plans	AASHTOGuide (Lev.1)
STRUC-TURE_ NUMBER _008	OWNER _022	STRUCT -URE_ KIND _043A	STRUCT -URE_ TYPE _043B	YEAR_ BUILT _027	MAX_ SPAN _LEN_MT _048	DECK_ WIDTH _MT_052	Connection _type	Min_num _connections	Min_ Size _inch	Wl_ kN_m	FvMax _kN_m
*Bridge ID	Owner	Super-structure kind	Material /design	Year Constructed	Longest Span Length (m)	Deck Width (m)	Dowels(2), Anchor Bolts (1) or Both(3)	Min num of Dowels /Anchors	Small-est Dowel /Anchor Size (in)	Superstructure Weight Per Unit Length(kN/m)	Vertical Force (kN/m)
2900050	1	4	2	1958	33.2	27.7	1	2	1	313.66	583.6
2900150	1	4	2	1973	32	9.9	1	2	1	57.22	76.6
2900240	1	5	2	1975	22.8	10.5	3	1	1	71.64	380.4

* (note): Three selected bridges are shown for illustration purpose only.

7.3 ArcMap File

An ArcMap file, including all shapefiles, has been created for GDOT to conveniently review and synthesize the study outcomes. The study team strongly believes that a graphical representation of coastal bridges vulnerable for each of the five hurricane categories will assist GDOT in making informed decisions. For example, an option of displaying vulnerable bridges by the owners is provided, as described in Section 6.3.1. Figures presented in Sections 4 through 6 are created using this ArcMap file.

8. DESIGN CONSIDERATIONS, VALIDATIONS, AND IMPROVEMENTS

8.1 Design Considerations, Mitigation, and Discussions

One of the critical considerations in the design of coastal bridges is elevation. It is first and foremost important to emphasize that bridges should be elevated based on a review of the most up-to-date storm water elevation information. The other important consideration is structural adequacy. In connecting superstructures to substructures, anchor bolts or dowels are used as part of bearing connections. The dowels and anchor bolts have been identified as most vulnerable elements in coastal bridges. However, the condition of anchor bolts such as corrosion was not considered in this study due to limited resources. Accurate information regarding condition states of each bridge elements, including anchor bolts, would be beneficial to reflect the condition of bridge elements in conducting a risk assessment in the future. Such information may become available through the GDOT's element-based inspection inventories.

Dowel connections are most commonly used for coastal bridges in Georgia. However, the bridges which are classified vulnerable and contain anchor bolt connections should be investigated in more detail. Increasing the size of anchor bolts may negatively affect the structural response and/or failure mechanism. A substructure failure could occur, which is generally more catastrophic than a superstructure failure because such failure is accompanied by a failure of multiple spans.

In bearing connections, dowels have been prevalently used. It is recommended to consider providing external restrainers in the form of stainless steel chain links and weather-protected (e.g., a protective sheath around) high-tension cables. It is important not to over-design the anchor bolts and external restrainers as they could have a negative impact on the structural

response of the substructure (or bridge piers). Shear keys should also be considered to prevent the lateral deck shifting failure.

Bridge decks are generally cast continuous over 2 or 3 simple-span precast concrete girders, and thus it is recommended evaluating such continuous concrete pour conditions in resisting hurricane-induced forces. This factor was not considered in the analyses presented in Sections 4 through 6. Therefore, a 3-dimensional finite element analysis is constructed in ANSYS (Version 18.1) as shown in Fig. 37 to evaluate the effect of a continuous concrete bridge deck in a simply-supported precast bridge failed by the Level-II analysis. Uplifting wave forces for Category 5 hurricanes are computed in accordance with the AASHTO Guide and are applied to the model. The results indicate that the consideration of continuous concrete deck pours in the model slightly reduces vertical reaction forces at intermediate supports. It is concluded that anchor bolts at the first and forth bents fail in tension whereas the anchor bolts at the second and third bents do not yield in the case analyzed. Therefore, it is feasible to consider providing external restrainers at the ends of every three spans where each continuous concrete deck pour terminates.

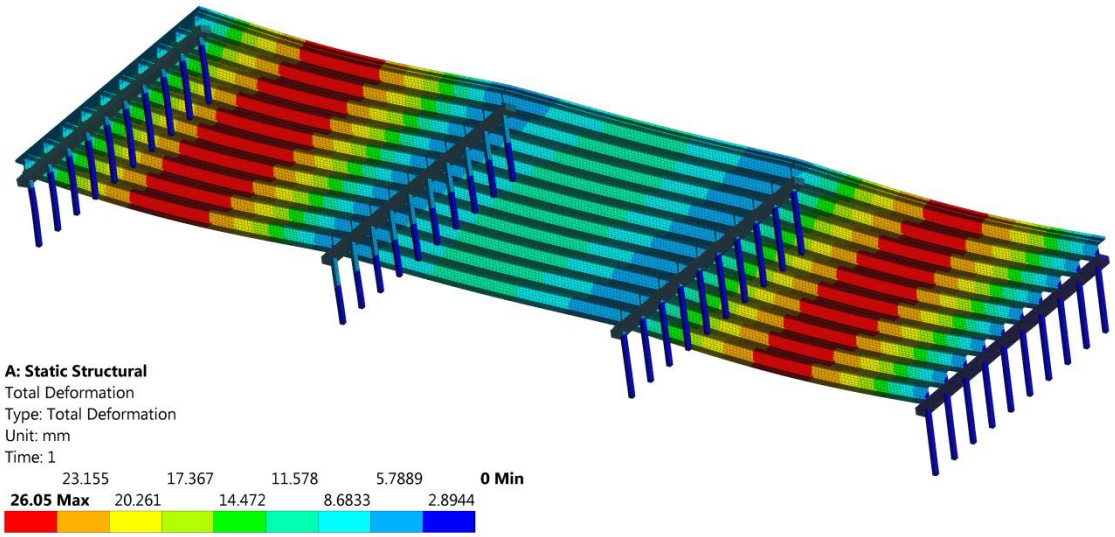

(a) Vertical displacement results of a 3-span bridge model, mm.

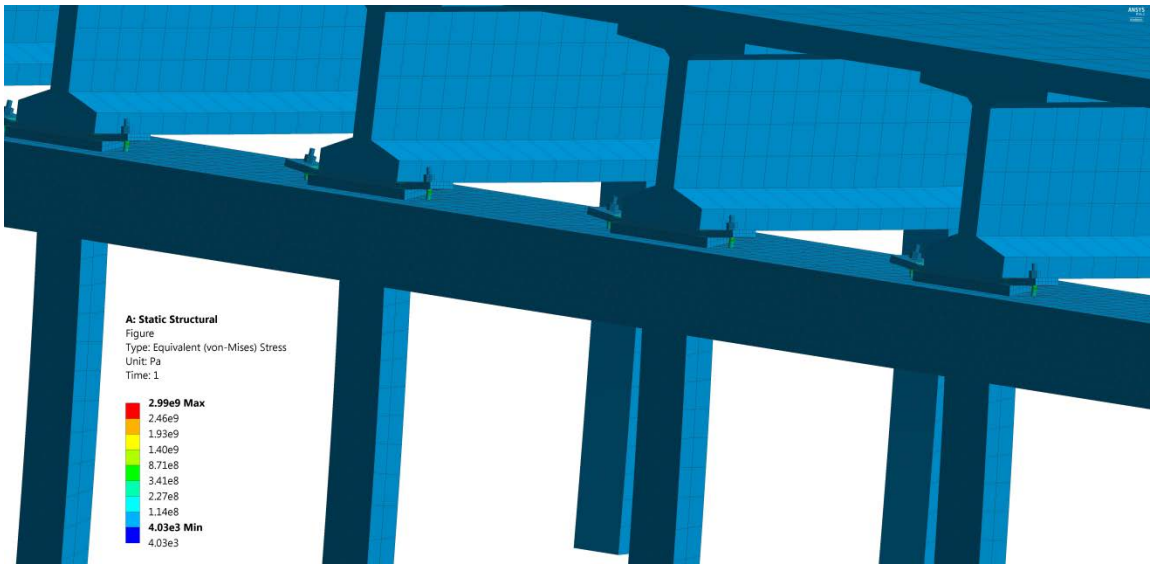

(b) Stress results at the first bent location (from the left), Pa.

Figure 37 – 3D Finite Element Analysis Model Reflecting a Continuous Deck Pour.

8.2 Validation Effort

The UGA research team visited the Transportation Management Center (TMC) on Friday afternoon, October 7, 2016 in order to monitor coastal bridges pending the arrival of Hurricane Matthew. Mark Demidovich and Binh Bui coordinated the meeting, and Mr. Demidovich made a workstation available for the team in TMC.

The research team initially planned to monitor multiple coastal bridges. However, a limited number of cameras were available in the coastal area as shown in Fig. 38. It was found that only seven cameras are available along I-95. Only six cams were in working condition, and the research team was able to monitor six bridges (mostly overpasses that are elevated). They were on a cellular connection (slow) whereas there were hundreds of cameras in the metro Atlanta area on a fiber connection (relatively faster). The team stayed at TMC through the night to monitor the six bridges; however, three cameras stopped working as the hurricane brushed Georgia. The team and TMC staff discussed that more cameras could be installed in the near future for monitoring GDOT's infrastructure (roads and bridges) as well as improving the 511 service in the coastal area.

(a) Screen capture of Hurricane Matthew.

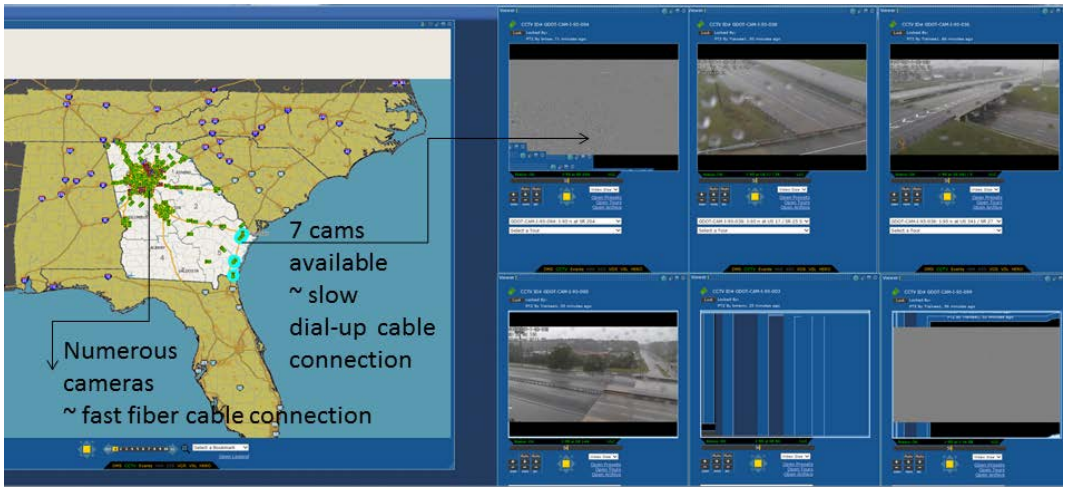

(b) Camera locations and views.

Figure 38 – TMC visit in October, 2016.

8.3 Future Improvements

Specific hurricane tracks most probable to occur in the Atlantic coast will need to be assessed (i.e., Level III assessment) such that the maximum SLOSH predictions will be replaced by less conservative storm water elevations in order not to yield overly conservative hurricane-induced wave forces. Furthermore, there is a need to monitor vulnerable coastal bridges during hurricane events by means of technology. For example, an installation of more traffic cameras in the coastal area should allow GDOT to improve its continuous monitoring capability.

9. SUMMARY AND CONCLUSIONS

A hurricane vulnerability assessment is conducted to determine the probability of failure of coastal bridges in Georgia. Coastal bridges show limited signs of vulnerability for Category 1 and Category 2 hurricanes. However, the number of vulnerable bridges significantly increase for major hurricanes, i.e., hurricanes with winds greater than 110 mph (category 3 or higher on the Saffir Simpson hurricane wind scale). The vulnerability of bridges in the hurricane evacuation route is mainly depicted by state-owned concrete bridges with super- and sub-structures connected by dowels.

In summary, the research team has provided GDOT with the ability to identify:

(1) coastal bridges which are at greatest risk of inundation or damage by a range of hurricane wind, surge, and wave loadings, spanning Category 1 to 5 events;

(2) bridge components (e.g., bearing connections with dowels and anchor bolts) which are vulnerable to hurricanes; and

(3) the suitability of the AASHTO Guide for future coastal bridge design.

The following sub-sections summarize the study findings from the initial screening (Section 4), Level-I analysis (Section 5), Level-II analysis (Sections 6.1- 6.3), and risk assessment (Section 6.4).

9.1 Potential Vulnerable Bridges by the Worst Scenario SLOSH Model

A vulnerability assessment was conducted using the worst-case (e.g., the upper threshold wind speed and the MOM SLOSH storm water elevations) hurricane scenarios for each of the five hurricane categories using the AASHTO Guide specification.

9.2 Initial Screening by Means of Storm Water Elevations

Based on the initial findings of this investigation:

- When a major hurricane lands, it is expected that more than 207 bridges and 66 culverts are to be submerged (or under water). This could indicate that the transportation network associated with the submerged bridges may not be functional. Over 60% of the coastal bridges are owned by the state.
- The surge elevation ranges between 1 m (3.3 ft) and 5 m (16.4 ft) for major hurricanes; therefore, the coastal bridges are considered to be in the body of shallow water, rather than deep water (e.g., bridges in Florida).

9.3 AASHTO Guide Level I Assessment

The failure mode in coastal bridges is mainly depicted by deck uplifting (or unseating) failures. The Level-I analysis is used to quantify the vertical wave forces. In this approach, it is assumed that failures occur in bearing connections, specifically in dowels and/or anchor bolts which are used to connect bridge superstructures to substructures, regardless of anchor/dowel capacity. Therefore, in this approach, the main wave force resisting component is the self-weight of bridge structures. Based on the findings of the Level-I investigation:

- The superstructure weight is not sufficient to prevent the bridge uplifting failure mode for major hurricanes (Category 3 or above). Using this approach, 227 bridges, over 35% of the coastal bridges, are anticipated to fail by Category 3 hurricanes, regardless of connection types, i.e., dowel and anchor bolt connections.

- The vulnerability assessment approach using the AASHTO's Level-I analysis method is appropriate to determine whether the weight of superstructure is sufficient to resist the vertical uplifting load induced by severe hurricanes.

- For major (Category 3 through 5) hurricanes, the controlling failure mode is deck uplifting. This failure mode is primarily attributed to dowels used in bearing connections which connect bridge superstructures to substructures.

- This simplified Level-I analysis method provides the most convenient and easiest way to assess the hurricane vulnerability because bridge self-weight is only considered for resisting hurricane induced wave forces while the tensile/shear capacity of anchor bolts is ignored.

9.4 AASHTO Guide Level II Assessment and Probabilities of Failure

A vulnerability assessment of coastal bridges was conducted using the NOAA's MOM SLOSH models for storm surge elevations and the AASHTO Guide. The primary failure mode observed in coastal bridges is depicted by deck uplifting failure due to bearing connections containing dowels. Based on the findings of this investigation, the following recommendations are provided:

- 173 and 22 bridges that are potentially vulnerable to major hurricanes pertain dowel and anchor bolt connections, respectively.
- Anchor bolt connections do not always warrant a protection from the bridge uplifting failure mode for major hurricanes (Category 3 or above). For Category 5 hurricanes, 39 bridges with anchor bolts are anticipated to fail (refer to Table 10).
- Over 65% of vulnerable bridges for major hurricanes (Category 3 or above) are state-owned bridges.
- Approximately 90% of vulnerable bridges are simply supported.
- 39 bridges identified vulnerable for Category 5 hurricanes are on the hurricane evacuation route.

9.5 Risk Assessment

A hurricane-hazard risk assessment of coastal bridges was conducted using the available hazard curve in an effort to predict the mean annual rate of return, AMR_{Bridge}, and identify bridges with a AMR_{Bridge} greater than 0.1. Seventeen bridges at comparatively high risk have been identified, and the bridge IDs are provided.

10. AASHTO GUIDE AND OTHER RECOMMENDATIONS

Using the AASHTO Guide was helpful throughout this investigation. The guide contains a structured method for computing wave forces. The equations recommended in the guide are clear and easy to follow for bridge engineers who may not have much experience in the design of coastal structures. In regards to recommended methods of analysis, each level of assessment is covered in detail. The AASHTO Guide also provides recommendations on how to determine the wind speed, wave height, period, and forces.

Based on the experience of conducting a vulnerability investigation using the AASHTO Guide, it is highly recommended for GDOT's adoption for critically important coastal bridges in Georgia, with the following additions/recommendations:

- A comprehensive vulnerability assessment could be very extensive, expensive, and time consuming. Precautions should be exercised when conducting Level I and Level II assessments because the results could yield overly conservative design. It is recommended that GDOT considers conducting the Level III assessment such that advanced numerical simulations of the sea state will be reflected, which usually starts with open sea modeling followed by shallow depth modeling, more advanced determination of wave parameters, and most plausible hurricane tracks, rather than using the worst scenario delineated from multiple hurricane tracks.

- It is very important to emphasize that coastal bridges should elevated based on a review of the most up-to-date storm water elevation information. It should be recognized that the

SLOSH MOM data is one of the storm surge elevation models available for such evaluation.

- It is recommended that heavier bridge super-structure systems be considered for coastal bridges. Increased deck thickness, deck overlays, and/or larger girder sections provide additional vertical resistance against hurricane-induced surge and wave loads due to gravity.

- It is also recommended that anchor bolts, rather than dowels, are desirable for bearing connection designs because they provide additional vertical resistance beyond the gravity action. However, dowels are commonly used in Georgia and are better protected from corrosion when embedded in concrete members. Stainless anchor bolts are also utilized at selected bridge locations although they are not always practical and easy to maintain. Therefore, it is necessary to study other types of super-to-substructure connections in order to allow the use of dowels while providing the means to resist vertical wave forces.

- It is very important to recognize that replacing dowels with anchor bolts is not always the best solution. An increase in the anchor bolt size may negatively affect the structural response by transferring hurricane-induced wave forces to the substructure and/or resulting in a substructure failure, which is considered more catastrophic than bearing connection failures. Therefore, it is critical to assess the effect of connection detail changes on the force transfer and failure mechanism for specific bridge types, details, and locations.

- It is also recommended that external restrainers (e.g., chains or cables) and shear keys are considered in conjunction with dowels for both existing and new bridges such that dowels are used for practical reason while the external retainers are used to provide additional tensile capacity needed to resist the hurricane induced forces. However, the capacity of such restrainers must be carefully assessed such that they do not negatively affect the force transfer mechanism.

- It is vital to calibrate and refine the vulnerability prediction model by monitoring bridges before/after future hurricane events. To accurately investigate the bridge performance and enhance the prediction model, it is recommended that the recovery effort and damage reports must be accurately documented during and after hurricane events. This includes, but not limited to, a documentation of storm water elevations, degree of damage in bridge elements, and bridge failure modes, if any, and related traffic information during re-entry or recovery effort.

- It is suggested that all construction documents be efficiently archived and easily accessible when vulnerability assessments are undertaken. This includes all design and construction drawings, rehabilitation history, bridge inspection reports, and other design information such as cross sectional properties of superstructures and super-to-substructure connection details.

- It is strongly recommended that detailed analyses for bridges with high-vulnerability and/or high-risk be conducted.

- For coastal bridges recently being built and to be constructed in the future, it is finally recommended to maintain a database of important parameters including the bridge elevation, cross section or weight per linear foot of span, and anchor or dowel size/quantity.

- It is highly recommended to develop a continuous monitoring program of coastal bridges in Georgia, in order to systematically identify signs of distress and failure modes (e.g., dowels and anchor bolts), if any, and recognize the most economical time for providing any rehabilitation, if needed.

- As GDOT inspects and maintains bridges, assessment of anchor bolts and dowels, if accessible, must be documented, because they are critical components for determining hurricane vulnerability. It is strongly recommended that GDOT develops a systematic design methodology for Georgia coastal bridges as it plans for future major repairs and replacements.

- At present, for coastal bridges in Georgia critically important to the safety of residents and economic well-being of the country, GDOT should consider designing anchor bolt connections utilizing the AASHTO Guide. Otherwise, it is deemed most practical to

design dowel connections and provide external restrainers at the ends of each span or every 2-3 spans where a continuous deck pour discontinues.

11. REFERENCES

1. Ataei, N., Stearns, M. C., Padgett, J. E. (2010) “Response Sensitivity and Probabilistic Damage Assessment of Coastal Bridges under Surge and Wave Loading,” Transportation Research Record: Journal of the Transportation Research Board, Vol. 2202 / 2010, pp. 93-101.
2. Ataei, N., and Padgett, J. E. (2012). "Probabilistic modeling of bridge deck unseating during hurricane events." *Journal of Bridge Engineering*, 18(4), 275-286.
3. American Association of State Highway and Transportation Officials (2008). Guide Specifications for Bridges Vulnerable to Coastal Storms. AASHTO, Washington, D.C.
4. Ataei, N. (2013). "Vulnerability Assessment of Coastal Bridges Subjected to Hurricane Events." Ph.D. dissertation, RICE UNIVERSITY, Houston, TX.
5. Baker J.W. (2015). “Efficient analytical fragility function fitting using dynamic structural analysis.” *Earthquake Spectra*. 2015;31:579-99.
6. Battjes, J. A. et al. (1987). “A reanalysis of the spectra observed in JONSWAP.” *Journal of Physical Oceanography*. 17(8), 1288-1295
7. Bouw, E. Gunther, H. Rosenthal, W., and Vincent, C. (1985). “Similarity of the wind wave spectrum in finite depth water: 1. Spectral form.” *Journal of Geophysical Research: Oceans*, 90(C1), 975-986.
8. Business in Savannah (2013). http://businessinsavannah.com/bis/2013-09-06/georgia-ports%E2%80%99-deepening-project-gathers-momentum#.UjdCd8akpkM. Updated in 2013. Accessed Sept. 15, 2013.
9. Casas-Prat M and Holthuijsen LH. (2010). “Short-term statistics of waves observed in deep water,” Journal of Geophysical Research: Oceans. 115.
10. Donelan, M. A., Hamilton, J., Hui, W. H. (1985). “Directional spectra of wind generated waves.” *Philosophical Transactions of the Royal Society of London A: Mathematical, Physical, and Engineering Sciences*, 315(1534), 509-562.
11. Douglass, S. L., Chen, Q., Olsen, J. M., Edge, B. L., and Brown, D. (2006) “Wave Forces on Bridge Decks.” Report by the Coastal Transportation Engineering Research and Education Center of the University of South Alabama to FHWA. Washington D.C. 74 pp.
12. Douglass, S. L., & Krolak, J. (2008). “Highways in the coastal environment.” Hydraulic Engineering Circular 25-Volume 1, FHWA Report No. FHWA-NHI-14-006.

13. Douglass, S. L., Webb, B. M., & Kilgore, R. (2014). Highways in the Coastal Environment: Assessing Extreme Events Hydraulic Engineering Circular No. 25 – Volume 2, FHWA Report No. FHWA-NHI-14-006.
14. FEMA Flood Maps (2014): http://msc.fema.gov/portal Accessed March 15, 2015.
15. Feng X, Tsimplis MN, Quartly GD, Yelland MJ. (2014), "Wave height analysis from 10 years of observations in the Norwegian Sea," Continental Shelf Research. 2014;72:47-56.
16. FHWA (2012-2017). Moving Ahead for Progress in the 21st Century (MAP-21). https://www.fhwa.dot.gov/map21/ Accessed July 5, 2017
17. FHWA (1995). Recording and Coding Guide for the Structure Inventory and Appraisal of the Nation's Bridges." Report No. FHWA-PD-96-001. https://www.fhwa.dot.gov/bridge/mtguide.pdf Accessed July 5, 2017
18. Forristall, G.Z. (1978). "On the statistical distribution of wave heights in a storm." Journal of Geophysical Research: Oceans. 83(23), 53-58.
19. GEMA (2013). http://www.gema.ga.gov/gemaohsv10.nsf/c6049b8deb5d38a185257726003-aa1dd/68ec9214ddb5b64a8525773500716735. Updated in 2013. Accessed Sept. 15, 2013.
20. Ghosh, J. (2013). "Parameterized Seismic Reliability Assessment and Life-Cycle Analysis of Aging Highway Bridges." Ph.D. Thesis, Rice University., Houston, TX.
21. Glukhovskiy BKH. (1961). "Study of wave attenuation with depth on the basis of correlation analysis." Meteorologiya i Gidrologiya, 22-30.
22. Gutierrez, C. M., Cresanti, R., and Jeffrey, W. A. (2006). "Performance of physical structures in Hurricane Katrina and Hurricane Rita: A reconnaissance report." *NIST Technical Note*, 1476.
23. Guikema, S., and Gardoni, P. (2009). "Reliability estimation for networks of reinforced concrete bridges." *Journal of Infrastructure Systems*, 15(2), 61-69.
24. Hasselmann K, Sell W, Ross D, Müller P. (1976). "A parametric wave prediction model. Journal of Physical Oceanography." Vol. 6, 200-28.
25. Hasselmann K, Barnett T, Bouws E, Carlson H, Cartwright D, Enke K, et al. (1973). Measurements of wind-wave growth and swell decay during the Joint North Sea Wave Project (JONSWAP). Deutches Hydrographisches Institute.
26. Karamlou, A., and Bocchini, P. (2015). "Computation of bridge seismic fragility by large - scale simulation for probabilistic resilience analysis." *Earthquake Engineering & Structural*

Dynamics, 44(12), 1959-1978.

27. Kameshwar, S., and Padgett, J. E. (2014). "Multi-hazard risk assessment of highway bridges subjected to earthquake and hurricane hazards." *Engineering Structures*, 78, 154-166.
28. Khelifa, A., Garrow, L., Higgins, M., and Meyer, M. (2013). “Impacts of Climate Change on Scour-Vulnerable Bridges: Assessment Based on HYRISK.” ASCE Journal of Infrastructure System, 19(2), 138–146.
29. Klopman G. (1996). “Extreme wave heights in shallow water,” Report H2486, WL| Delft Hydraulics. 1996.
30. Le Méhauté B, Lu C, Ulmer E. (1986). Transformation of statistical properties of shallow water waves. Proceedings the 1981 Conference on Wave Dynamics and Radio Probing of the Ocean Surface. 181-91.
31. Li, Y., Song, R., and Van De Lindt, J. W. (2014). "Collapse fragility of steel structures subjected to earthquake mainshock-aftershock sequences." *Journal of Structural Engineering*, 140(12), 04014095.
32. Longuet-Higgins, M.S. (1975). “On the joint distribution of the periods and amplitudes of sea waves,” Journal of Geophysical Research, 80(26), 88-94.
33. Longuet-Higgins, M.S. (1980). “On the distribution of the heights of sea waves: some effects of nonlinearity and finite band width”. Journal of Geophysical Research: Oceans. 85(15), 19-23.
34. Longuet-Higgins M.S. (1983). On the joint distribution of wave periods and amplitudes in a random wave field. Proceedings of the Royal Society of London A: Mathematical, Physical and Engineering Sciences: The Royal Society, 241-58.
35. Mazzoni, S., McKenna, F., Scott, M. H., and Fenves, G. L. (2006). “OpenSees command language manual.” Pacitif Earthquake Engineering Research (PEER) Center.
36. Naess A. (1985). “On the distribution of crest to trough wave heights,” Ocean Engineering. Vol. 12, 221-34.
37. Nayak S, Panchang V. (2015). “Coastal Wave-Height Statistics during Hurricane Ike,” Journal of Waterway, Port, Coastal, and Ocean Engineering, 142:04015026.
38. Nielson, B. G., and DesRoches, R. (2007). "Seismic fragility methodology for highway bridges using a component level approach." *Earthquake Engineering and Structural Dynamics*, 36(6), 823-839.

39. Nielson, B. and DesRoches, R. (2006). “Seismic fragility methodology for highway bridges using a component level approach.” Earthquake Engineering and Structural Dynamics, 36: 823-839.
40. NOAA Budget Blue Book (2013). http://www.corporateservices.noaa.gov/nbo/fy14_bluebook/FINALnoaaBlueBook_2014_Web_Full.pdf. Updated January 2013, Accessed Sept. 15, 2013.
41. NOAA SLOSH Model: http://www.nhc.noaa.gov/surge/slosh.php. Updated in 2014. Accessed March 15, 2017.
42. NYC (2013). NYC Report, “A STRONGER, MORE RESILIENT NEW YORK - Sandy and Its Impact.” June 2013.
43. Ochi, M. K., & Hubble, E. N. (1977). Six-parameter wave spectra. In *Coastal Engineering 1976* (pp. 301-328).
44. Okeil, A. M., & Cai, C. S. (2008). Survey of short-and medium-span bridge damage induced by Hurricane Katrina. *Journal of Bridge Engineering*, *13*(4), 377-387.
45. Padgett, J. E., Spiller, A., Arnold, C. (2009). "Statistical Analysis of Coastal Bridge Vulnerability using Empirical Evidence from Hurricane Katrina," Structure and Infrastructure Engineering, Special Issue on Monitoring, Modelling, and Assessment of Structural Deterioration in Marine Environments, DOI:10.1080/15732470902855343.
46. Padgett, J. E., and DesRoches, R. (2008). "Methodology for the development of analytical fragility curves for retrofitted bridges." *Earthquake Engineering and Structural Dynamics*, 37(8), 1157-1174.
47. Padgett, J. E., Nielson, B. G., and DesRoches, R. (2008b). "Selection of optimal intensity measures in probabilistic seismic demand models of highway bridge portfolios." *Earthquake Eng. and Str. Dyn.*, 37(5), 711-726.
48. Pierson WJ, Moskowitz L. (1964). “A proposed spectral form for fully developed wind seas based on the similarity theory of SA Kitaigorodskii,” Journal of geophysical research. Vol. 69, 5181-90.
49. Saeidpour, A. (2017). “Fragility Analysis of Coastal Bridges Susceptiable to Hurricances Incoporating Uncertainties in Extreme Wave Parameters By Means of Wave Spectra and Enhancement of Vulnerability Assessment Methodologies.” PhD disseration. The University of Georgia, Athens, GA, August, 2017.

50. Simpson, R. H., and Saffir, H. (1974). "The hurricane disaster potential scale." *Weatherwise*, 27(8), 169.
51. Sheppard, D. M., and Marin, J. (2009). "Wave loading on bridge decks." *FDOT report*, FDOT, Gainesville, FL.
52. Simiu, E., Vickery, P., & Kareem, A. (2007). Relation between Saffir–Simpson hurricane scale wind speeds and peak 3-s gust speeds over open terrain. Journal of Structural Engineering, 133(7), 1043-1045.
53. Standford, Scott S. (2012). Risk Assessment of Florida's Coastal Bridges Exposed to Hurricane-Induced Storm Surge Wave Forces. M.S. Thesis, The Florida State University, 2012, pp. 95.
54. Sturm et al. (2004) "Laboratory and 3D Numerical Modeling with Field Monitoring of Regional Bridge Scour in Georgia." Report No. FHWA-GA-04-2002 prepared for the Georgia Department of Transportation and FHWA.
55. Stamey, T. C. (1996). "USGS Summary of Data-Collection Activities and Effects of Flooding From Tropical Storm Alberto in Parts of Georgia, Alabama, and Florida, July 1994", USGS Report No. 96-228 prepared in cooperation with GDOT.
56. Tayfun M.A. (1983). "Nonlinear effects on the distribution of crest-to-trough wave heights," Ocean Engineering, Vol. 10. 97-106.
57. The United States Department of Transportation (2013). http://www.dot.gov/briefing-room/us-transportation-secretary-lahood-announces-additional-76-million-emergency-relief. Updated in 2013. Accessed Oct. 02, 2014.
58. Tavares, D. H., Suescun, J. R., Paultre, P., and Padgett, J. E. (2013). "Seismic fragility of a highway bridge in quebec." *Journal of Bridge Engineering*, 18(11), 1131-1139.
59. Tayfun M.A., Fedele F. (2007). "Wave-height distributions and nonlinear effects," Ocean engineering. Vol. 34, 1631-49.
60. Thornton EB, Guza RT. (1983). "Transformation of wave height distribution," Journal of Geophysical Research: Oceans, Vol. 88, 5925-38.
61. Towashiraporn, P. (2004). "Building seismic fragilities using response surface metamodels." Ph.D. Thesis, Geogria Institue of Technology, Atlanta, GA.
62. U.S. ARMY CORPS OF ENGINEERS (2009). Emergency Operations Plan Incident Annex A, Appendix 5, Historic Storm Tide Elevations, U.S. Army Corps of Engineers Savannah

District in Cooperation with the Chatham Emergency Management Agency, Chatham County, July 2009. http://www.chathamemergency.org/documents/EOP%20INCIDENT-%20ANNEX%20A%20APPENDIX%205%20HISTORIC%20STORM%20TIDE%20ELEVATIONS%20REV0709.pdf. Accessed May 1, 2017.

63. USACE (1984). Shore protection manual. Army Engineer Waterways Experiment Station, Vicksburg, MS. 2v, US Army Corps of Engineers.
64. USEngineering Solutions (2017). BridgeWatch Software. http://www.usengineeringsolutions.com/bridge-watch/ Accessed July 5, 2017.
65. Vickery, Peter J., et al. (2009). "US hurricane wind speed risk and uncertainty." *Journal of structural engineering*, 135(3), 301-320.

A list of electronic submittals:

1. A WORD/PDF copy of the RP15-01 final report.

2. A GIS file that incorporates the project findings presented in this report.

3. An Excel file summarizing the surveyed elevations and raw data used for this project.

4. A PDF copy of M.S. thesis.

5. A PDF copy of Ph.D. dissertation.

6. Journal publications and manuscripts.